

"Crystallization in Multi-phase Polymer Systems"

Crystallization behaviour of polymer nanocomposites

V. P. Cyras, D. A. D'Amico and L. B. Manfredi

Instituto de Investigaciones en Ciencia y Tecnología de Materiales (INTEMA), UNMdP,
CONICET, Facultad de Ingeniería, Av. Juan B Justo 4302, B7608FDQ,
Mar del Plata, Argentina

Abstract

This chapter is an overview of the effect of the different nanofillers in the crystallization performance of polymer matrices. The most relevant nanocomposites were classified according to the nature of the reinforcement.

In general, it was reported that the way of processing highly affect the crystal sizes, crystalline structure and the degree of crystallinity of semicrystalline polymer nanocomposites, then modifying the performance of the material. Therefore, the influence of different crystallization processes on barrier, thermal stability, dynamic or mechanical properties of nanocomposites was described. Moreover, it was observed that the crystallization mechanism of polymers in the nanocomposites strongly depends on the intrinsic characteristics of the nanoparticles and the matrix, and in consequence the dispersion of the filler in the matrix.

This chapter focuses on the studies about the effect of different types of nanofillers on several aspects of polymer crystallization, such as kinetics, crystal structure, nucleation effect as well as spherulitic grow and morphology.

1. Introduction

During the last decade polymer nanocomposites appeared as a new class of materials which have attracted the attention of researchers and industrial area. The

incorporation of certain nanoparticles makes the nanocomposites to gain a series of unique properties, such as optical, mechanical, thermal, electrical, magnetic, surface wear, etc. The main factor is the large surface area to volume ratio of the nanoparticles, which is also expected to have a marked effect on the crystallization behavior of polymer. The processing of polymer (extrusion, injection molding, and film blowing) generally involves non-isothermal crystallization conditions so, the knowledge of the parameters affecting crystallization is crucial for the optimization of the processing conditions and the properties of the end product [1]. In semicrystalline polymers several properties are highly affected by the degree of crystallinity and the morphology (crystal sizes and crystalline structure) which depend on the conditions under which the crystallization process was carried out. The main known effects during crystallization are heterogeneous nucleation, transcrystallinity and epitaxy[2]. Solid surfaces existent in a polymer melt induce heterogeneous nucleation by reducing critical enthalpy for nucleation at the melt/solid interface. With the large surface area of nanoparticles, the chain mobility near the particle surface could widely affect crystallization. Additionally, the interaction between the polymer and the nanoparticle surface affect the polymer morphology [3].

In this chapter, recent progress made in understanding the crystallization in polymer nanocomposites is described. It is mainly structured by the principal nanofillers used, by focusing on the effect nanofillers have on various aspects of crystallization such as crystallization kinetics, crystal structure and nucleation effect.

2. Crystallization in polymer nanocomposites

2.1. Polymer nanolayered nanocomposites

Among the nanometric fillers used in the manufacture of nanocomposites, clays are the most extensively used industrially as a reinforcement of polymeric materials for the last 30 years [4,5]. These nanoparticles have dimensions of the order of 1 nanometer of thickness and hundred nanometers in its axial direction [6,7]. However, the tendency to form agglomerates within the matrix is preponderant as the filler becomes smaller, so it is difficult to disperse the clay uniformly in the polymer matrix [5].

Generally, clay may be classified into two categories: natural and synthetic clays. Figure 1 shows the classification of natural clays. They are basically composed of alternating sheets of SiO_2 and AlO_6 units in ratios of 1:1 (kaolinite), 2:1 (montmorillonite (MMT) and vermiculite (VM)) and 2:2 (chlorite) [8].

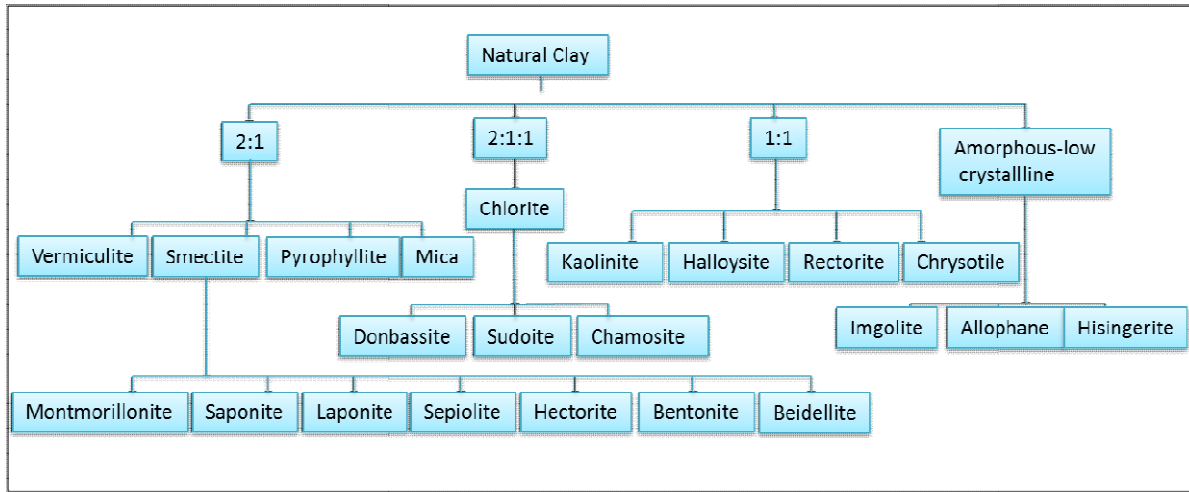


Figure 1. Classification of natural clays.

The feasibility of obtaining nanocomposite polymer / clay with improved properties is determined by the final morphology obtained. For this purpose, the ideal morphology would be one in which the nanofiller is exfoliated, so that the clay sheets are thoroughly and uniformly dispersed in polymeric matrix [9]. However, the tendency to agglomerate of the particles (due to the large surface area per volume unit) becomes difficult to obtain this type of microstructure. At the same time, the hydrophilic character of the clays and the predominantly hydrophobic character of polymeric matrix become necessary to modify one of these components in order to increase the interactions between them, to improve the interface and also obtain the type of morphology and the desired properties [10]. Table 1 shows several types of nanocomposites based on polymer and different clays. These nanocomposites have been processing with modified and unmodified clays by typical compounding techniques.

Table 1. Nanocomposites based on polymer/clay.

Polymer	Clay	Clay modification	Processing method	Crystallization features	Reference
Polyhydroxybutyrate (PHB)	MMT	Ionic exchange, grafting with a chlorine silane.	Solvent casting	No effect on nucleation activity. Same crystal morphology in PHB and its nanocomposites. No significance changes in Avrami exponents among the different nanocomposites and the pristine polymer matrix.	[11,12]
Polyhydroxybutyrate-co-valerate (PHBV)	MMT, Halloysite (Hal)	Chemical bonding of APTES	Melt compounding	Multiple melting peaks, presence of low molecular weight chains led to the formation of these less perfect crystals with a wide range of sizes. Degradation of the polymer during processing in the presence of the silane.	[13]
Polylactic-acid (PLA)	MMT	Ionic exchange	Melt compounding, solvent casting.	Exfoliated nanocomposites: no effect on nucleation activity (1%), increase on the crystallization rate, resulting in big spherulite size. Intercalated nanocomposites: increase on nucleation activity with the clay content, resulting in small spherulite size.	[14, 15, 16,17]
Polytrimethylene terephthalate (PTT)	MMT	Ionic exchange	Melt-press	Increase on nucleation activity and spherulitic rate with the clay content. For the PTT nanocomposites, the n values are clearly larger than that of the neat PTT. This can be indicative of a more complicated nucleation type and crystal growth form of the spherulites for the PTT nanocomposites.	[18]
Polyethylene	MMT,	Ionic exchange	Melt	Clay induces the higher crystallization rates and lower activation	[19]

terephthalate (PET)	laponite.		compounding	energy, the clay aspect ratio had a minor effect, compared to dispersion and type of organic modifier of clay platelets.	
	Layered double hydroxide (LDH)	Ionic exchange	Solvent casting	A nucleation effect was induced by the LDH nanoparticles, independent of the clay loadings. The values of Avrami parameter remain almost constant, therefore the nanoparticles had little effect on the 3D growth pattern of the spherulites.	[20]
Polypropylene (PP)	MMT.	Ionic exchange	Melt compounding	The number of spherulites increased and their size decreased when clay was incorporated, which is also an indication of the heterogeneous nucleating behavior. Faster spherulitic growth and increasing K_g (nucleation parameter).	[21,22]
Polyethylene (PE)	MMT, Vermiculite	Ionic exchange, chemical bonding acid treatment and MA grafting	Melt compounding, In situ polymerization	Exfoliated silicate layers acted as effective nucleation sites for the secondary nucleus. The crystallization of nanocomposites was characterized by two distinct regimes, I and II (Lauritzen Hoffman theory). The fold surface energy values were found to decrease with increasing clay content, up to 2% in regime I. Further increasing the VMT content resulted in a slight increase of the fold surface energy.	[23,24,25]
Polyamide-6	MMT	Ionic exchange	In situ polymerization	The crystallization rate of N6 is faster in the presence of clay compared to pure N6. Nylon 6 crystallizes exclusively in the γ -form in the nanocomposite.	[26, 27]

When a clay is added to a semicrystalline polymer, the clay platelets may have different effects on the crystallization, depending also on the way in which the nanocomposite has been processed. Nano-thick and micrometre-long clay plates can serve as heterogeneous nucleation centers due to the high interfacial energy generated by the chemical incompatibility between the clay and the polymer. In addition it should be noted that each platelet provides a huge surface area per unit volume.

As Table 1 shown, clays have been added in synthetic polymers (PE, PP, PET, PBT, PTT, Polyamide-6) and natural (PHB and PHBV, PLA) to improve their mechanical and barrier properties. In such cases, clays must be organically modified, due to the hydrophobic character of these polymers matrix, as it was mentioned above. Also, with the addition of the clay, it is expected to increase the crystallization rate, since they can act as nucleating agents.

Smith and Vasanthan [18] studied the effect of a commercial organo-modified montmorillonite (Cloisite[®] 15A) on isothermal and non-isothermal melt crystallization behavior of PTT by differential scanning calorimetry (DSC) experiments and polarized light microscopy (POM). Also they evaluated the roll of nanoclay on conformational changes during melt crystallization using FTIR spectroscopy. They found that, when the PTT crystallizes from the melt, the size of the spherulites appears to depend on the crystallization temperature and the clay loading. The effect of temperature on the crystallization rate of polymers has already been studied and understood. In contrast, the effect of the clays on the crystallization rate has not been fully understood. In the Smith and Vasanthan work, the spherulite size decreases with increasing clay content from 0% to 10% at each melt crystallization temperature. It is also apparent that the smaller spherulites (~30–80 μm) are mixed with larger spherulites (~100 μm) at the lower melt crystallization temperatures, whereas the smaller spherulite size is prevalent, especially at higher loading and at higher melt crystallization temperatures (Figure 2).

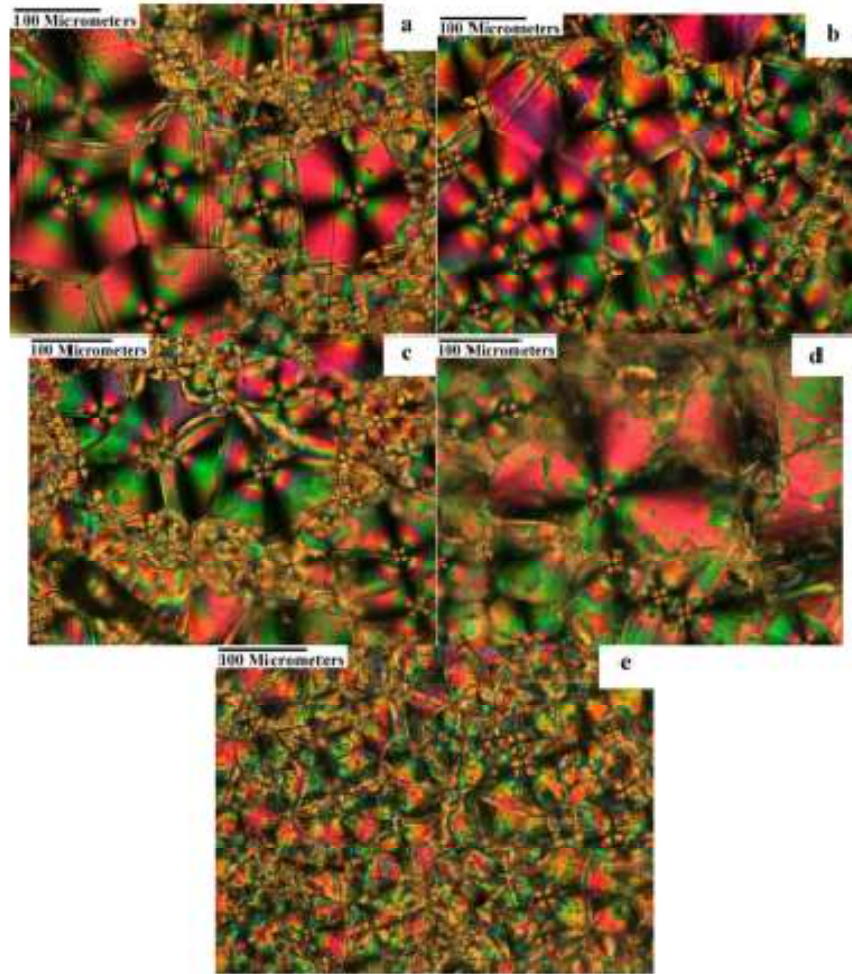


Figure 2. Polarized light microscopy photographs of 110°C melt crystallized neat PTT and PTT nanocomposites films with various nanoclay loadings: (a) neat PTT, (b) 1%, (c) 2%, (d) 5% and (e) 10%.

Figure 3 shows the clay dispersion for the exfoliated nanocomposite of PTT and Cloisite 15A. The size of the spherulite is apparently controlled by the amount of nuclei and the rate of crystallization. These results would indicate that the nanoclay particles in the PTT matrix act as nuclei for crystallization and enhance the rate of crystallization.

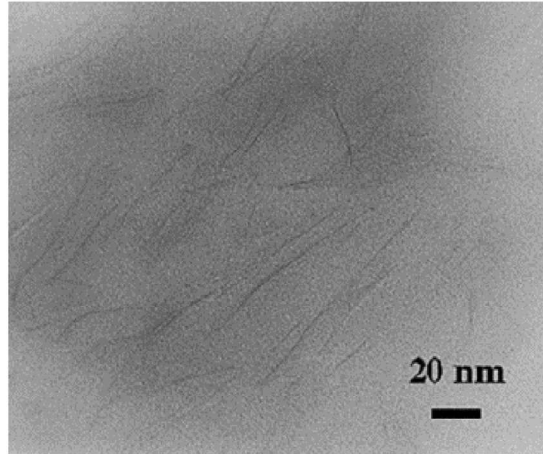


Figure 3. Transmission electron micrograph of PTT with 5% Cloisite 15A.

In the same way Yuan et al. [23] and Perez et al. [21] have studied the crystallization of nanocomposites based on the synthetic polymers PE and PP, respectively. The former have studied the influence of nanoclay particles on the non-isothermal crystallization behavior of intercalated polyethylene prepared by melt-compounding. In their work, it is observed that the crystallization peak temperature at cooling of PE/clay nanocomposites is slightly but consistently higher than that of neat PE. When the clay content increased the half-time ($t_{0.5}$) for crystallization decreased, implying a nucleating role of nanoclay platelets. They also found that the overall crystallinity of PE decreased with the addition of nanoclay. They suggest that the lower crystallinity may be ascribed to the lower mobility of polymer chains in the PE matrix, which resulted from the presence of nanoclay particles. It is likely that the dispersed clay particles hinder the formation of large crystalline domains in the restricted and confined space. They studied the effective activation energy by Kissinger method and higher values in the nanocomposites than the neat polymer were found. When the clay was added, they found two mutually opposite effects on the crystallization behavior of PE nanocomposites: nucleating ability, the decrease of half-time indicates the lower free energy barrier for PE/clay nanocomposites compared to neat PE, and growth retardation associated to the activation energy for the transport of crystalline units across the phase, which is related to the content and dispersion state of clay.

Pérez et al. [21] have studied the effect of clay nanoparticles, unmodified and modified (Cloisite 30B (C30B) and Cloisite 10A (C10A)), on the overall crystallization

behavior of polypropylene by means of DSC and POM. Besides, they also analyzed the change produced by the compatibility between the filler and the matrix, by using hydrophobic clays and incorporating PP grafted with maleic anhydride (PP-g-MA). They observed a nucleating effect of clay nanoparticles, evidenced on the induction time, half-crystallization time and overall crystallization time calculated through the measure of the crystallization temperature (T_p), melting temperature (T_m). In addition, POM showed that the number of spherulites increased and their size decreased when clay was incorporated, which is also an indication of the heterogeneous nucleating behaviour of such particles. The effect was also related with the matrix/clay compatibility. In all cases the nucleating effect was more evident in nanocomposite with unmodified clay.

Cao et al. [20] studied the effect of organo anion-intercalated layered double hydroxide (LDH_DDA) on PET crystallization, another type of clay nanoparticles which had significant effects on the PET non-isothermal crystallization kinetics. A nucleation effect was observed by the addition of LDH_DDA nanoparticles. The PET/LDH_DDA nanocomposites exhibited dramatically increased crystallization rate relative to pure PET matrix. They calculated the apparent activation energy (E_a) of crystallization in the nanocomposites with different clay loads (1, 3 and 5%) and pure PET. The E_a of the PET/LDH_DDA nanocomposites were much lower than that of pure PET, and even decreases with the increase of the LDH_DDA content, demonstrating that LDH_DDA nanofillers acted as good nucleating agents by significantly lowering the crystallization E_a .

Maiti and Okamoto [26] studied in detail the crystallization behavior of pure Polyamide 6 (N6) and its nanocomposite with montmorillonite. In this type of polymer unmodified clay can be used due to the hydrophilic character of the matrix. Light scattering experiments revealed that the crystallization rate of nanocomposites was faster than that of pure N6. They found that N6 crystallizes exclusively in the γ -form in the nanocomposite because of the epitaxial crystallization, which is also revealed from the transmission electron microscopic images (sandwiched structure) of the crystallized sample (Figure 4).

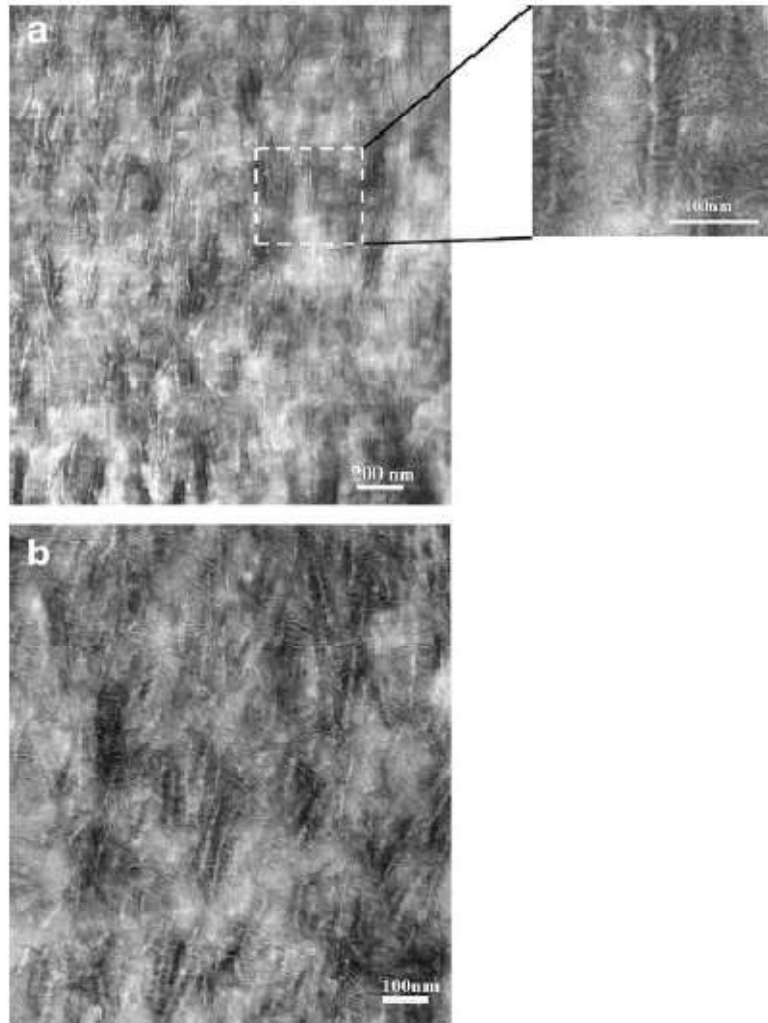


Figure 4. Bright field TEM images of N6C3.7 crystallized at (a) 170°C and (b) 215°C. The enlarged part shown (Fig. 4(a)) forms the indicated lamellae in the original image. The black strip inside the white part is an individual MMT particle. Fig. 4(b) shows the typical shish-kebab type of structure.

The nucleation rate was so high in the case of the N6 nanocomposites that the spherulite sizes become very small. Here, it should be mentioned that nylon 6 exhibited nice spherulites over a wide range of crystallization temperatures. Apparently 3.7 wt.% clay was sufficient to nucleate the whole bulk and as a result the spherulitic pattern disappeared but the system crystallizes very quickly. A unique sandwiched morphology was observed for the epitaxial crystallization of nylon 6 in the presence of clay layers, which can explain

well the reason for high crystallization rates and the formation of only a γ -form in the nanocomposite.

So far, clays have a nucleating effect on the crystallization of great part of polymers, but it has also been reported in the literature that clays have a null or retarding effect on crystallization depending on the polymer matrix, dispersion state and modification. D'Amico et al. [11, 12] and Papageorgiou et al. [19] calculated the nucleation activity by using the Dobreva method [28] in montmorillonite modified with different organic surfactants (tributylhexadecylphosphonium bromide and alkyl ammonium salts) in PHB and PET nanocomposites. They found a slight or no nucleating effect of the clays in these polymers; this behavior can be attributed to the clay dispersion and chemical compatibility between the polymer matrix and the organic modifier employed. The nucleation activity decreases (more active filler) when a good dispersion (exfoliated nanocomposite) is achieved, due to the increase in the polymer/clay surface. On the other hand, when a lack of physical interaction between the polymer and the inorganic surface of clay platelets is obtained, due to the steric hindrance generated by the organic surfactant, the nucleation activity is in the proximity of 1 indicating an inert filler.

Lai et al. [14] studied the effect of an organic-modified MMT on the crystallization behavior of a nearly amorphous PLA matrix. PLA/clay exfoliated nanocomposites were obtained by adding only with 1 phr of clay by melt-blending process. Based on SEM and TEM pictures, the highly exfoliated platelets produced a relatively large interfacial area between the clay platelet and PLA matrix, which resulted in a comprehensively plasticized interfacial region. The highly plasticized interfacial region and the well dispersed clay platelets with high aspect ratio caused a decrease in the spherulite nucleation behavior of the PLA. The exfoliated nanocomposite even has lower nucleation behavior than the neat PLA. Krikorian and Pochan [16] studied the crystallization behavior of PLLA adding organic-modified MMT (Cloisite 30B and Cloisite 10A) by using optical microscope, DSC and infrared spectroscopy. They found that when a high degree of filler-polymer miscibility and good dispersion of filler are present, nucleation properties of the organoclay are low relative to the less miscible organoclay. Consequently, the overall crystallization rate was increased in the intercalated system and slightly retarded in the exfoliated system. Surprisingly, spherulite growth rates were significantly increased relative to the bulk in the

fully exfoliated nanocomposite. The overall crystallinity degree and the size of crystalline domains decreased by addition of organoclays and are the lowest in the fully exfoliated case. Spherulite nucleation was low when the clay organic modifier is highly miscible and very well dispersed in PLLA (exfoliated nanocomposite). The bulk crystallization rate was slower, and the extent of crystallinity was much lower than that of neat PLLA. On the other hand, spherulite radial growth rate was significantly higher compared to that of neat polymer (Figure 5).

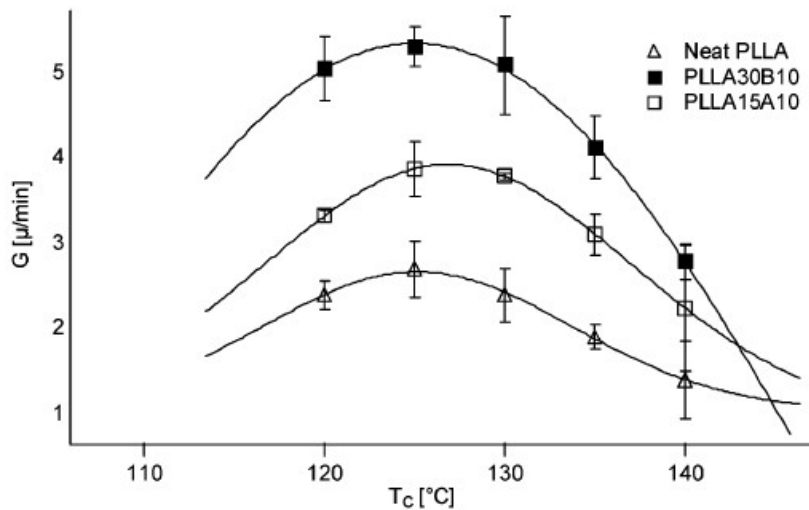


Figure 5. Spherulite growth rate (G) as a function of crystallization temperature (T_c) for neat PLLA, PLLA with 10 wt% of Cloisite 30B and Cloisite 15A.

The above mentioned behavior might be due to a superstructure templating effect associated with fully exfoliated clay platelets that, sequentially, hinders local lamellar crystallization and leads to the least degree of crystallinity observed (Figure 6a). Low spherulite nucleation behavior combined with higher radial growth rate resulted in much bigger final spherulite sizes. In contrast, in nanocomposites with an intercalated morphology due to lower miscibility between the polymer matrix and the organic modifier, the clay acts as an effective nucleating agent leading to increased bulk crystallization rates. This results in much finer spherulites and a higher overall degree of crystallinity as compared to the exfoliated case (Figure 6b).

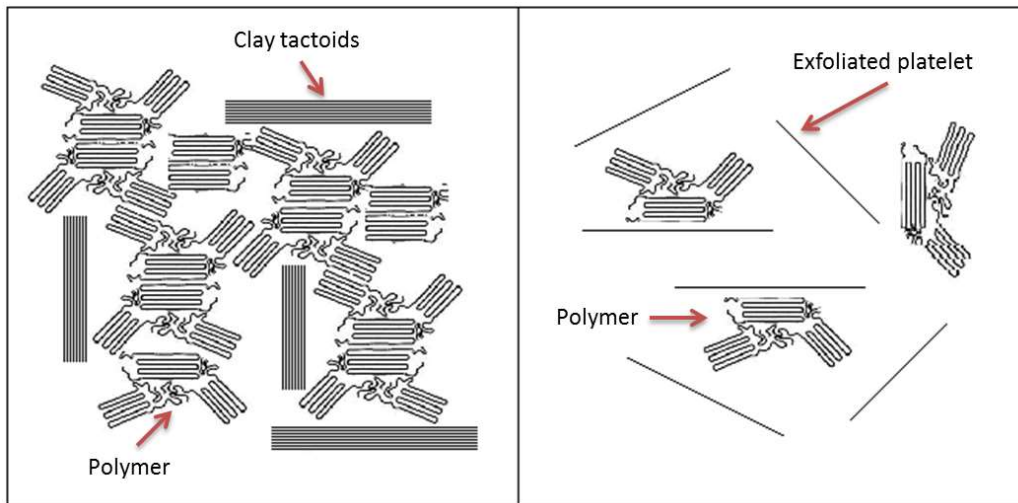


Figure 6. Relationship between dispersion, miscibility and crystallization in polymer/clay nanocomposites.

In most of the aforementioned works, it was reported that the clays did not significantly affect the crystalline morphology. In addition, in the nanocomposites where the clays acted as nucleating agents and increased the overall crystallinity, the tensile modulus also increased, except for the Nylon-6 nanocomposites, where the clays induced the γ -form crystals, which have a smaller tensile modulus than the α -form crystals. In this nanocomposite, the increase on the tensile modulus is manifested by the effect of the addition of a material (MMT) with greater tensile modulus than the polymer matrix one, without morphological modifications leading to more rigid materials. Particularly, in the PLA nanocomposites with low clay load the highly exfoliated platelets created a quite large interfacial area between the clay and PLA matrix, which resulted in a widely plasticized interfacial region. This region and the properly dispersed clay platelets with high aspect ratio, improved the multiple shear-banding which promote the plastic deformation and substantial shear yielding behavior. It also led to a decrease in the spherulite nucleation behavior of the PLA. In contrast, when the clay was added at higher amounts, the intercalated form was the structure predominant, and clay acted as rigid filler.

1.1. Metal–polymer nanocomposites

Xia et al. [29] studied the non-isothermal crystallization behavior of copper/low density polyethylene (Cu/LDPE) nanocomposites prepared by melt-blending technique in a single-screw extruder. They observed that the nanocomposites and the pure LDPE, have a different crystalline structure. The DSC results showed that the incorporation of 13 wt.% copper nanoparticles decreases the melting temperature but increases the crystallization temperature of LDPE, and also lowers the crystallinity degree of the matrix. The decrease of the melting temperatures was explained considering the less ordered crystalline structure and lower crystallinity degree of the LDPE in the nanocomposites; the increase of the crystallization temperatures was related with the nucleating effect of the copper particles, increasing the nucleation ratio. Additionally, the copper nanoparticles hinder the motion of the polymer chains segments, retarding the crystal growth and thus, decrease the crystallinity degree of the nanocomposite. It was also observed that the incorporation of the copper nanoparticles improves the thermal stability of the LDPE, but the increase of the thermal stability of the Cu/LDPE nanocomposites will decrease when the content of the copper nanoparticles is more than 2 wt.% (Figure 7).

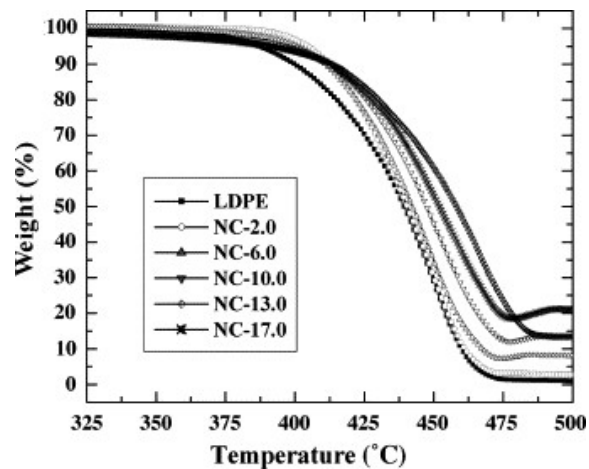


Figure 7. TGA thermograms of pure LDPE and its Cu/LDPE nanocomposites with various content of copper nanoparticles.

On the other hand, Ma et al. [3] studied the effect of TiO₂ nanoparticle surfaces on the crystalline structure of LDPE. The nanoparticle surface was varied from hydrophilic (as-received) to less hydrophilic (dried) or more hydrophilic (polar silane treated). They found that the nanoparticles, with the various different surface conditions investigated, did not modify the degree of LDPE crystallinity, the unit cell dimensions, the average lamellar thickness, or spherulite size. It was concluded that the average lamellar thickness (between 20 and 40 nm) did not change much with the addition of nanoparticles having different surface conditions by means of the phase AFM images of the neat LDPE and the nanocomposite with the silane treated nanoparticles (AR-TiO₂). DSC observations were consistent with that conclusion. However, the nanoparticles did affect the internal arrangement of intraspherulitic crystalline aggregates. The nanocomposites containing the nanoparticles surface more hydrophilic exhibited the highest internal disorder and the most poorly developed spherulite structure. This was attributed to the comparable size between the spherulite size and the nanoparticles aggregates.

The effect of the addition of TiO₂ nanoparticles on the crystallization process of high density polyethylene (HDPE) matrix was studied by Olmos et al. [2]. They demonstrated that high energy ball milling process (HEBM) is a good method to prepare nanocomposites of well dispersed TiO₂ nanoparticles (2 wt.%) in a HDPE matrix. The HEBM process induced the reduction of crystallinity of the polymer although a double crystallization process was observed; however, when nanoparticles are present, the appearance of a metastable monoclinic phase was favored, and the crystallinity degree of HDPE increases with milling time, from about a 60% of crystals when the mixture was milled for 1 h to about a 70% when the mixture was milled for 10 h. Atomic force microscopy (AFM) images clearly showed how well dispersed were the TiO₂ nanoparticles in the polymer matrix and how they are localized exactly between the lamellas, which evidences that they actually do not act as nucleating agents (Figure 8). Additionally, they also showed that the nanoparticles induced a more homogeneous crystallization of HDPE leading to denser spherulites with thicker lamellae.

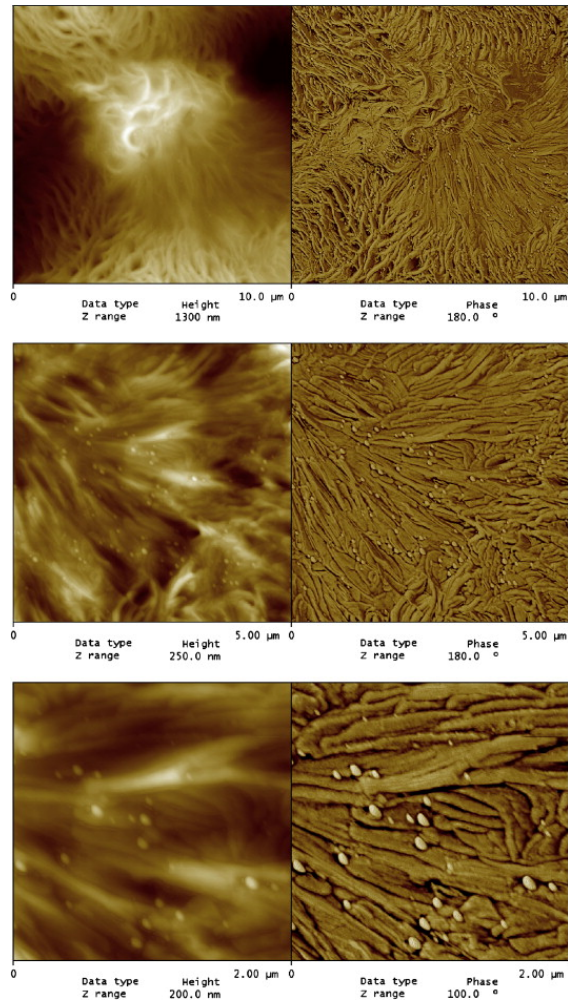


Figure 8. Morphology of the HDPE/TiO₂ milled for 10 h obtained by topographic and phase AFM images (left and right respectively).

Additionally, Huang et al. [30] studied the non-isothermal and isothermal crystallization behavior of poly(ethylene oxide) (PEO)/MXene nanocomposites. Their final aim is to fabricate solid polymer electrolytes (SPEs) for energy storage. PEO is widely used in SPEs, due to its high dielectric constant and strong lithium ion solvating capability. MXenes are a new family of 2D transition metal carbides and/or nitrides, which have unique electrical, thermal and mechanical properties. In this work, MXene Ti₃C₂T_x (where T is a surface termination) was used to obtain nanocomposites using a solution blending method. The crystalline structure of PEO did not change with the addition of MXene as verified by the wide angle X-ray dispersion (WAXD) experiments, which also showed that

the $Ti_3C_2T_x$ layers were exfoliated. They observed that very low contents of $Ti_3C_2T_x$ accelerated PEO crystallization, but PEO crystallization was inhibited with the loading increasing. The fastest crystallization rate was observed at 0.5 wt.%MXene content, which was attributed to the competition of nucleation and confinement effect of the 2D filler (Figure 9).

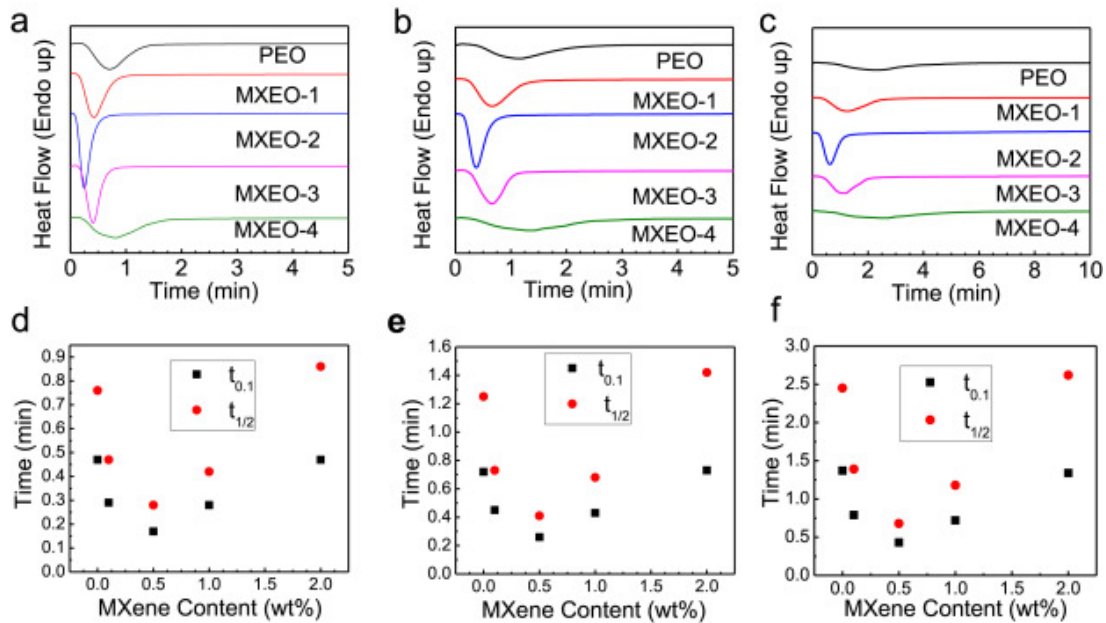


Figure 9. Isothermal crystallization behavior of nanocomposites tested herein. (a-c) Isothermal DSC thermograms at 46°C, 48°C and 50°C. (d-f) functional dependence of $t_{0.5}$ and $t_{0.1}$ on MXene content. MXEO-1 to 4: nanocomposites with 0.1%, 0.5%, 1% and 2% MXene by weight, respectively.

1.2. Carbon Nanotube based nanocomposites

One of the most promising nanocomposites are the ones based on polymers and carbon nanotubes (CNTs). CNTs possess many unique properties such as high strength and modulus, thermal and electrical conductivities, as well as high aspect ratio. Nevertheless, it is very difficult to disperse the CNTs in a polymeric matrix due to their large surface areas and high Van der Waals forces among themselves, which tend to form aggregates. Chemical modification of CNTs creating acidic sites on their surface, such as carboxylic, carbonyl, and hydroxyl groups, significantly enhance the dispersion of the CNTs into the

polymer matrix [31]. It was reported that a small amount of well-dispersed CNTs could significantly improve various properties of polymer matrices, such as mechanical strength and modulus, thermal stability, crystallization rate, electronic conductivity, etc. [32].

The effect of multi-walled carbon nanotubes (MWNTs) on the non-isothermal crystallization behavior of MWNTs/polyamide 6 (PA6) nanocomposites prepared via a melt-blending process was studied applying the Avrami, Ozawa and Mo methods by Li et al. [33]. The results showed that the MWNTs acted as effective nucleation agents in PA6. However the crystallization rate of nanocomposites obtained was lower than that of the neat PA6. The MWNTs accelerated the PA6 nucleation but hindered the diffusion and aligned array of the polymer chains resulting in a slower crystallization rate of PA6. Thus, the presence of MWNTs influenced the mechanism of nucleation and the growth of PA6 crystallites.

Chen and Wu [31] studied the isothermal and non-isothermal crystallization kinetics of nylon 6 and nylon 6/functionalized multi-walled carbon nanotubes (f-MWCNT) nanocomposites. The MWCNT were functionalized introducing carboxylic acid groups at their local defect sites and thus improving the dispersion of the f-MWCNT in solution. They observed that the activation energy (E_a) of nylon 6 widely decreased by adding 1 wt % f-MWCNT into the polymer, suggesting that small amount of f-MWCNT possibly induces the heterogeneous nucleation. However, the addition of more quantities of f-MWCNT increased the activation energy because of the reduction of the transportation ability of polymer chains during crystallization process. In the case of non-isothermal crystallization, 3 wt.% f-MWCNT produced more heterogeneous nucleation, decreasing the E_a . Those results suggest that the dominant factor of isothermal and non-isothermal crystalline formation for nylon 6/f-MWCNT nanocomposites with high loadings of f-MWCNT is the crystal growth and nucleation mechanism, respectively. Then, in order to understand the effect of functional groups on the crystallization behavior of nylon 6 the authors fabricated f-MWCNT containing different weight ratio of functional groups on the surface or sidewall of MWCNT [34]. They found that the overall isothermal crystallization rates of nylon 6 increased as well as the activation energy of the polymer extensively decreased by adding 1 and 3 wt% f-MWCNT with different weight ratios of functional groups into the nylon 6. The apparent crystallite sizes of the nanocomposites decrease with

increasing weight ratio of f-MWCNT and the functional groups on the surface of f-MWCNT. These results suggested that the addition of f-MWCNT induced the heterogeneous nucleation decreasing the activation energy as well as the chain arrangement.

The crystallization behavior of nanocomposites based on polyethylene and single wall carbon nanotubes (SWNT) were also studied. They were obtained by a new hot-coagulation method which enables high SWNT loadings (up to 30 wt.%) with good distribution [35]. The Avrami model applied to thermal results showed that SWNT nucleates PE crystal growth and accelerates the crystallization rate while reducing the crystal dimensionality from spherulitic to disk-shaped.

Kim et al. [36] demonstrated that the non-isothermal crystallization behavior of poly(ethylene 2,6-naphthalate) (PEN) nanocomposites was strongly dependent on the presence of the modified carbon nanotube (CNT) and cooling rate. The nanocomposites prepared with the modified CNT showed a uniform dispersion of the nanoparticles in the PEN matrix as well as an increased interfacial adhesion between the nanotubes and the polymer, as compared to the untreated CNT. The mechanical properties of the PEN nanocomposites were significantly enhanced with the introduction of very small quantity of CNT and this enhancing effect was more pronounced in the nanocomposites with the modified CNT nanocomposites as compared to the untreated one. The improvement in the mechanical properties was attributed to good interfacial adhesion between the m-CNT and the polymer as well as uniform dispersion of the nanoparticles. Combined Avrami and Ozawa analysis was found to be effective in describing the non-isothermal crystallization of the PEN nanocomposites in the presence of the modified CNT. The variations of the nucleation activity and activation energy for crystallization reflected the enhancement of crystallization of the PEN nanocomposites induced by the modified CNT. Inversely, crystallization process of poly(ethylene oxide) (PEO) slowed down in presence of single walled carbon nanotubes (compatibilized by a lithium based surfactant) [37]. They showed that the PEO chains in the nanocomposites stiffen in presence of lithium dodecyl sulfate (LDS) with an increased energy barrier associated with the nucleation and crystal growth, and the nanotubes further act as a barrier to chain transport or enhance the efficacy of the LDS action. The polymer chains move towards local nucleation sites which yield thinner

crystal lamellae in spite of a slow crystallization process. Figure 10 shows the structural organization of the nanocomposites.

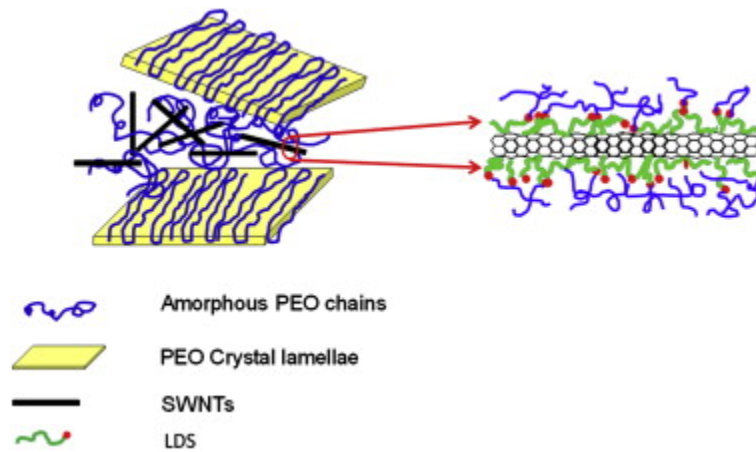


Figure 10. Structural organization in SWNTs-LDS-PEO nanocomposite system. Li based surfactants compatibilize the nanocomposite by acting as bridges between SWNTs and PEO. Due to Li^+ -PEO complexation and the barrier offered by SWNTs to chain diffusion to the growing lamellae, PEO crystals are formed away from nanotubes. The nanotubes are, thus, preferentially surrounded by amorphous PEO chains.

Lim et al. [38] reported that the addition of MWCNT could affect the non-isothermal crystallization kinetics of poly(vinylidene fluoride) (PVDF), but it did not change the crystalline polymorphs of the polymer at all. A kinetic equation for the non-isothermal crystallization was employed to analyze the crystallization behavior of the nanocomposites. The Avrami exponent indicated a spherulite morphology for the PVDF crystallites and that the presence of MWCNT caused an heterogeneous nucleation. It was attributed to a large number of nuclei (MWCNT) and also confirmed by POM (Figure 11).

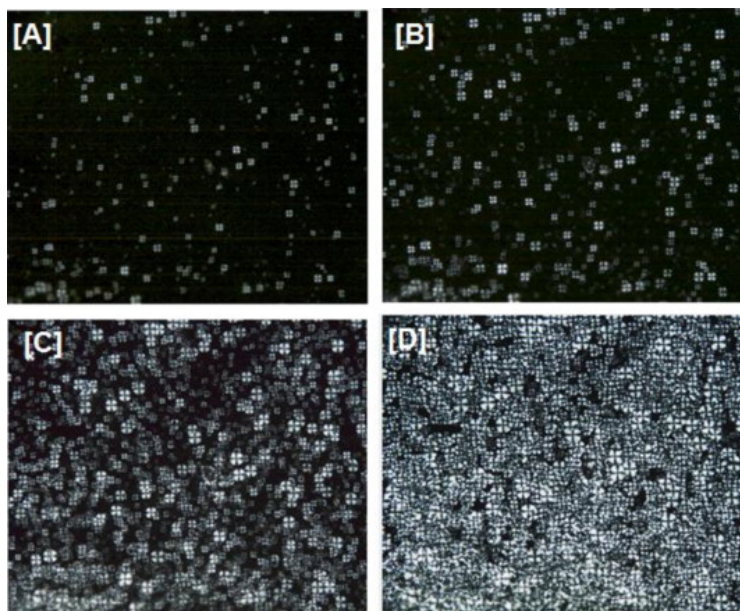


Figure 11. POM images of PVDF/MWCNT(0.1wt.%) at cooling rate, 4 °C/min [A] 143 °C [B] 142 °C [C] 141 °C [D] 140 °C (magnification x400).

Additionally, a wide variety of works were done about the analysis of the crystallization behavior of nanocomposites based on biodegradable polymers and carbon nanotubes. The isothermal crystallization of poly(ϵ -caprolactone) (PCL)/MWNT composites was studied by Wu et al. [39]. They reported that the addition of carboxylic groups containing multiwalled carbon nanotube (c-MWNTs) into PCL solution produced strongly heterogeneous nucleation induced by a change in the crystal growth process. The PCL activation energy significantly decreased by adding 0.25 wt.% c-MWNT and then increased with increasing c-MWNT content. Moreover, Jana and Cho [40], studied the non-isothermal crystallization behavior of poly(ϵ -caprolactone) (PCL)-grafted multi-walled carbon nanotubes (f-MWNTs). It was observed that the f-MWNTs into the PCL molecules induced heterogeneous nucleation and the crystal growth process was significantly affected. The crystallinity of composites decreased with the addition of f-MWNTs, likely due to the occurrence of more heterogeneous nucleation. The activation energy for PCL crystallization was significantly reduced with the addition of 2 wt.% f-MWNTs and slightly increased with increasing nanoparticles content. The nucleating action of MWNTs in the crystallization process was corroborated by POM. The experimental data were also

analyzed using various kinetic models e.g., Avrami, Tobin, Ozawa, etc. which described the experimental data for both the crystallization and melting processes fairly well.

A novel approach to induce crystallization in biodegradable poly(butylene succinate) (PBS)/single-walled carbon nanotube (SWCNT) nanocomposites was developed by Tan et al. [41]. The nanocomposites were obtained through covalent bonding (hydrolysis) and physical blend between PBS and acyl aminopropyltriethoxysilane functionalized SWCNT (SWCNT-APTES). From the DSC cooling and heating curves for PBS and PBS/SWCNT-APTES nanocomposites they observed that the crystallization temperature of all the nanocomposites were higher than that of neat PBS, and increased with the increase of the nanotube content, indicating that the SWCNTs served as the nucleating agent and promoted the crystallization rate of PBS (Figure 12). The double crystallization peak observed in the curve of the PBS/SWCNT-APTES (1%,hydrolyzed) nanocomposites was related to the agglomeration of the particles causing that some PBS chains which were so far away from a nanotube surface crystallizes at the same rate that pure PBS. They concluded that the incorporation of SWCNT-APTES enhanced the crystallization of the PBS in the nanocomposites due to the heterogeneous nucleation effect.

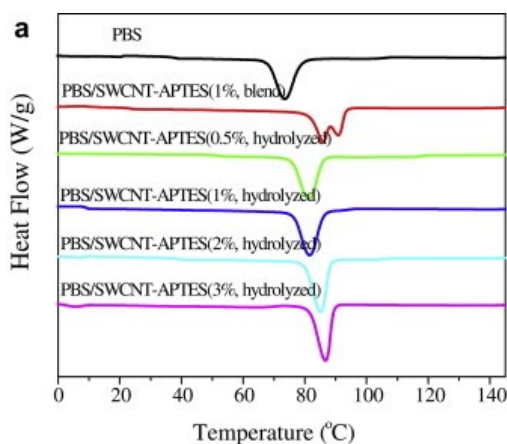


Figure 12. DSC thermograms of neat PBS and its nanocomposites from the melt (cooling).

More recently, Zeng et al. [32] incorporated functionalized MWCNTs into PBS through solution coagulation to fabricate CNTs filled PBS nanocomposites. MWCNTs were non-covalently functionalized by surface wrapping of poly(sodium 4-styrenesulfonate) (PSS) with the aid of ultrasound. DSC indicated that the melt

crystallization temperature of PBS was improved by 14°C with addition of only 0.05 wt.% nanoparticles. Additionally, the nanocomposites showed a significant improvement in the crystallization temperature with further increasing MWCNT content up to 0.5 %, which was attributed to the nucleating effect of the nanoparticles. The spherulitic morphology of neat PBS and its nanocomposites were corroborated by POM. A single melting peak was observed for the neat PBS, while all nanocomposites showed two melting peaks with a main peak close to that of neat PBS and a small peak at lower temperature than that of neat PBS. The small peak was ascribed to the melting of unstable crystals formed at higher temperature as the onset crystallization temperatures of the nanocomposites were much higher than that of neat PBS, due to the nucleating effect. Significant improvement in electrical conductivity occurred at CNT loading of 0.3 wt%, due to the formation of a conductive path with PBS matrix. Both the yield strength and Young's modulus of PBS were apparently reinforced by incorporation of functionalized CNTs, while the elongation at break was reduced with increasing CNT loading.

The combined effect of the addition of MWCNT and silver nanoparticles on the crystallization kinetics of PBS was studied by Papageorgiou et al. [42]. The nanocomposites were prepared by the solvent evaporation method showed a remarkable nucleating activity of the nanoparticles. Silver nanoparticles show the most enhanced crystallization kinetics. This was confirmed by conventional techniques such as POM (Figure 13) and DSC as well as differential fast scanning calorimetry (DFSC), which was employed in order to identify the temperature range of heterogeneous nucleation caused by both nanofillers. The recrystallization behavior of PBS and its nanocomposites was distinct from all other polymers studied so far as only the previously crystallized part of the material was able to recrystallize, independently on the available large number of nuclei. Since full melting of small crystals at low temperatures was observed this highlights the importance of ordered structures remaining in the polymer melt. On cooling from the melt the neat polymer did not crystallize at rates higher than 70 K/s, while the nanocomposites needed rates of 500 K/s and 300 K/s for silver and MWCNT, respectively. Below 280 K the crystallization kinetics of the matrix was almost the same with the nanocomposite samples. The nucleation mechanism changes at 280 K from heterogeneous to homogeneous.

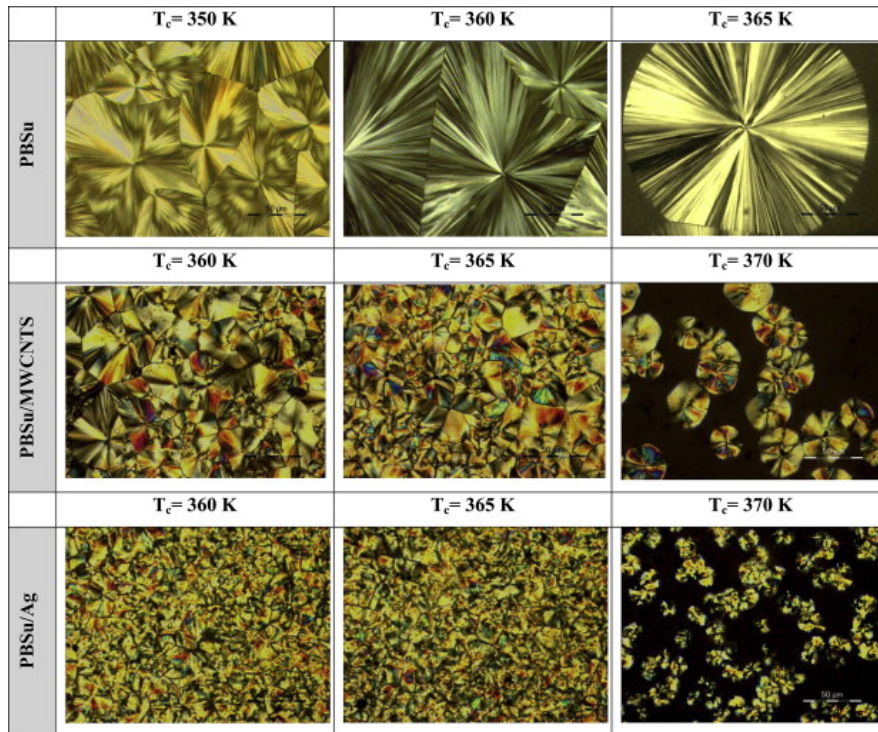


Figure 13. POM images of PBS and nanocomposites. The scale bar in all photographs is 50 μm .

The isothermal melt crystallization kinetics of poly(3-hydroxybutyrate) (PHB)/MWNTs nanocomposites was studied by Xu and Qiu[43]. The effect of different loadings of multiwalled carbon nanotubes containing carboxylic groups (f-MWNTs) on the non-isothermally melting behavior of PHB was studied. Both SEM and TEM observations indicated a fine and homogeneous dispersion of f-MWNTs throughout the PHB matrix. The study of the isothermal melt crystallization kinetics revealed that the overall crystallization rates are faster in the PHB/f-MWNTs nanocomposites than in neat PHB at a given crystallization temperature (T_c); furthermore, the overall crystallization rates decreased with increasing T_c for both neat PHB and the PHB/f-MWNTs nanocomposites. The acceleration of isothermal crystallization process of PHB in the nanocomposites was attributed to the heterogeneous nucleation effect of f-MWNTs. It was also reported that the addition of f-MWNTs does not modify the crystal structure of PHB in the nanocomposites.

1.1. Calcium carbonate nanocomposites

Precipitated calcium carbonate (CaCO_3), is one of the most usually employed nanofiller for polymers. Inorganic particulate fillers have been employed to improve properties and/or lower costs of polymer products. It was reported an enhancement in mechanical properties such as modulus, ductility and impact strength of polymers with the nano CaCO_3 addition. Moreover, the nonisothermal crystallization kinetics of CaCO_3 based polymer composites has also been the subject of large number of studies [44].

Supaphol et al. [45] prepared syndiotactic polypropylene filled with calcium carbonate (s-PP/ CaCO_3) in a twin-screw extruder. The effect of CaCO_3 with varying particle sizes (1.9, 2.8 and 10.5 μm), contents (0–40 wt.%), and types of surface modification (uncoated, stearic acid-coated and paraffin-coated) on crystallization and melting behavior of s-PP based nanocomposites was studied. Non-isothermal crystallization studies showed that the nanoparticles act as a nucleating agent for s-PP. The crystallization temperature increased with the CaCO_3 content and decreasing particle size. Surface coating of CaCO_3 particles with stearic acid and paraffin reduced the nucleating ability of the particles. So, the nucleating efficiency of CaCO_3 for s-PP depends strongly on its purity, type of surface treatment and average particle size. In general, the tensile strength of s-PP/ CaCO_3 compounds was found to decrease while Young's modulus increased, with increasing CaCO_3 content, probably due to the poor interfacial adhesion between the nanoparticles and the polymer. The average size of CaCO_3 particles did not appear to affect the tensile strength markedly. Both types of surface treatment on nanoparticles reduced tensile strength and Young's modulus, but improved impact resistance.

Avella et al. [44] studied the effect of the different shape of CaCO_3 nanoparticles, spherical (S) and elongated (E), on the thermal and crystallization behavior of isotactic polypropylene. The nanocomposites were prepared by melt mixing followed by compression molding. An improvement in the interfacial adhesion between the nanoparticles and the iPP as well as an increment in the glass transition temperature and the thermal stability of the material was reached covering the CaCO_3 with a polypropylene-g-maleic anhydride copolymer. They observed that the covered nanoparticles were efficient nucleating agents for iPP, and the overall crystallization rate resulted higher than original iPP. The presence of at least 3 wt.% CaCO_3 induced crystallization of iPP to start at higher temperatures, being the effect slightly dependent on the aspect ratio of the nanoparticles

(Figure 14). Moreover, Avella et al. (2006) performed an exhaustive investigation of the influence of the crystal modification of CaCO_3 nanoparticles and compatibilizers on the crystallization behavior of iPP. The calorimetric and optical studies showed that the coating agent used (polypropylene-g-maleic anhydride copolymer (PPMA), or fatty acids (FA)) widely affects the nucleating ability of the nanoparticles, but has a very slightly influence on crystal growth rate. The CaCO_3 coated with the graft copolymer promoted the onset of crystallization in iPP, whereas the nanoparticles coated with fatty acids resulted in a delay of the crystallization rate of iPP. It was attributed to the physical state of the coating and to the dissolution of heterogeneities in the polypropylene matrix by fatty acids. On the other hand, a very weak influence of both shape and crystal modification (calcite and aragonite (AR)) of CaCO_3 was observed, being the interfacial modifier the main factor affecting crystallization of iPP (Figure 15).

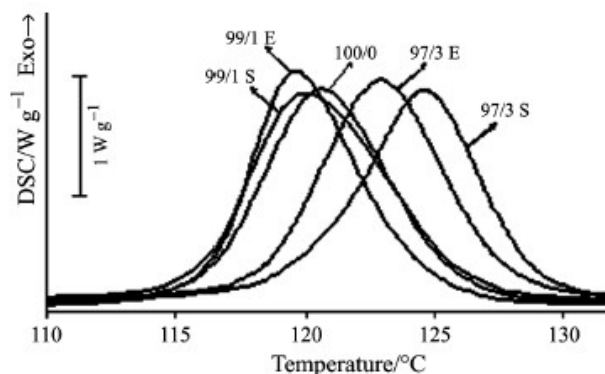


Figure 14. DSC thermoanalytical curves of iPP/ CaCO_3 nanocomposites at various compositions, measured during cooling from the melt at $8^\circ\text{C}/\text{min}$.

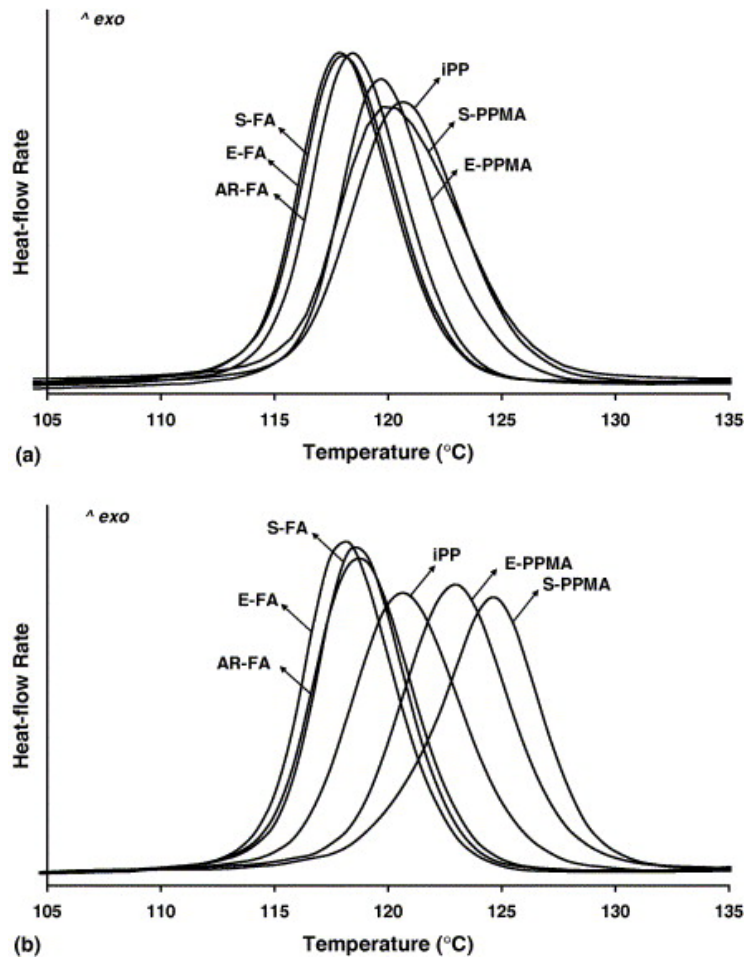


Figure 15. DSC thermoanalytical curves of iPP/CaCO₃ nanocomposites crystallized at 8°C/min containing: (a) 1% and (b) 3% of filler.

The effect of nanoparticle surface treatment on non-isothermal crystallization behavior of PP/CaCO₃ nanocomposites was studied by Wan et al. [47]. The CaCO₃ nanoparticles were surface-modified with various contents of aluminates coupling agent. Jeziorny and Mo methods showed that the crystallization temperature of the nanocomposites increased due to the heterogeneous nucleation of the surface-treated nanoparticles. The surface-treated nanoparticles had a strong nucleating activity, which caused the decrease of the activation energy of the nanocomposites. It was estimated by Dobreva and Kissinger's methods, respectively. It was reported that the Liu model seemed to be more suitable to describe the non-isothermal crystallization kinetics of HDPE, which was compared to the behavior of both a maleic anhydride-modified HDPE (manPE) and a CaCO₃nanocomposite[48]. The crystallization rate followed the order:

HDPE/CaCO₃>HDPE/manPE/CaCO₃> HDPE/manPE> HDPE. The effective activation energy was analyzed by the Friedman equation and the values of K_g and U* for non-isothermal crystallization were estimated by Vyazovkin's method. These results indicated that the addition of maleic anhydride groups and CaCO₃ tend to promote the nucleation of spherulites on their surfaces and lead to epitaxial growth of the crystallites. Moreover, the presence of the well-dispersed CaCO₃ particles and manPE may hinder the transport of the molecule chains resulting in a decrease of the crystallization growth rate. In the same way, Run et al. [49] applied the modified Avrami equation and Ozawa theory to the DSC data in order to study the non-isothermal crystallization behavior of poly(trimethylene terephthalate) (PTT)/CaCO₃nanocomposites prepared by melt-compounded. They found that the nanoparticles acted as nucleation agent, accelerated the crystallization rate by decreasing the activation energy. The nanocomposite with 2 wt.% CaCO₃ exhibited a maximum improvement both on the crystallinity and the crystallization rate. The Avrami and the Ozawa exponents, n and m of the nanocomposites, were higher than those of neat PTT. It suggested a more complicated interaction between the polymer chains and the nanoparticles producing changes in the nucleation mode and the crystal growth dimension. The optical micrographs showed that relatively smaller uniform spherulites were formed in nanocomposites compared with neat PTT. Moreover, the dimension of the crystal greatly decreased with increasing the nanoparticles content. CaCO₃ nanoparticles also exhibited a pronounced effect as a heterogeneous nucleating agent and enhances the crystallization rate of poly(ethylene terephthalate) [50].

Deshmukh et al. [1] studied the non-isothermal crystallization kinetics of poly(butylene terephthalate) (PBT)/nano calcium carbonate (CaCO₃) composites prepared by melt blending, containing 2, 5 and 10 wt.% of CaCO₃. Melt crystallization data from DSC was successfully described by macrokinetic models like modified Avrami and Liu and Mo. They showed the dependence of crystallization rate on CaCO₃ content: up to 5 wt.% of nanoparticles greatly accelerated the crystallization rate, whereas higher filler content reduced the crystallization rate. Effective activation energy values calculated by Friedman method corroborated these findings (Figure 16). Additionally, it was observed by POM that the spherulites size decreased as increased the filler content. They concluded that small amount of nanoCaCO₃ exhibits a combination of accelerating and limiting effects on

the crystallization of PBT depending on the filler content. Low amount of CaCO_3 acts as a nucleating agent and accelerates the rate of crystallization, whereas higher loadings increase the nucleation density but restrict the mobility of polymer chains and retard the growth process.

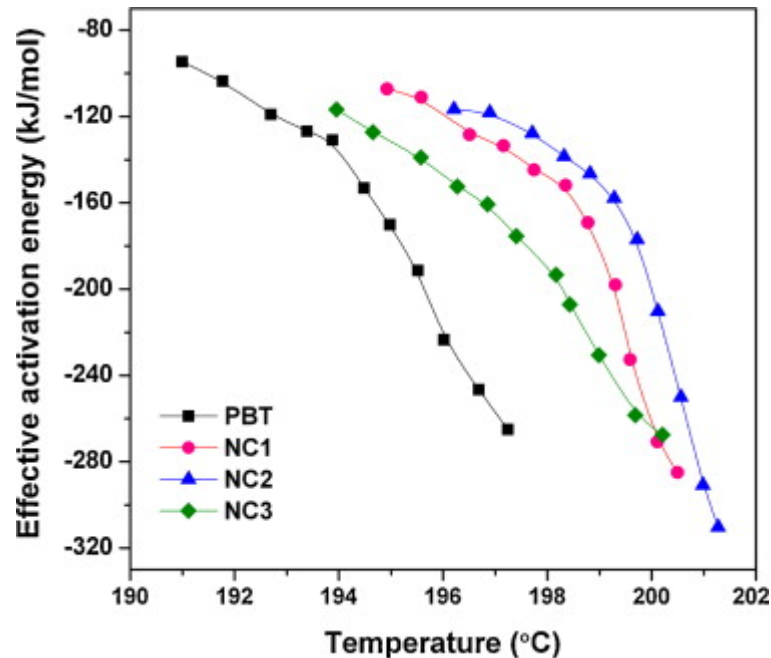


Figure 16. Effective activation energy as a function of temperature for PBT and its composites.

1.2. Silica nanocomposites

Silica (SiO_2) is another type of inorganic particles that are widely used as reinforcing agents of polymers. Surface of the nanoparticles are usually modified in order to promote their uniform dispersion into the polymer as well as to improve their interaction with the organic matrix. Different and sometimes contradictory results have been mentioned about the effect of SiO_2 nanoparticles on crystallization rate of semicrystalline polymers.

Rong et al. [51] reported that SiO_2 exhibits some nucleation effect on the crystallization rate of PP matrix though the addition of the nanoparticles does not greatly influence the whole crystalline features of the polymer. Papageorgiou et al. [52] studied the isothermal and non-isothermal crystallization kinetics of isotactic polypropylene

(PP)/surface-treated fumed SiO₂ nanocomposites. They reported that isothermal crystallization rates of i-PP-fumed silica nanocomposites increased with increasing filler content up to 7.5 wt.%. The modified Avrami method and the analysis of Mo were satisfactorily applied to model the non-isothermal crystallization results. The effective energy barrier for non-isothermal crystallization varied with the degree of conversion and the presence of filler. Moreover, the nucleation activity of the silica nanoparticles increased with the silica amount up to 7.5 wt.% (Figure 17).

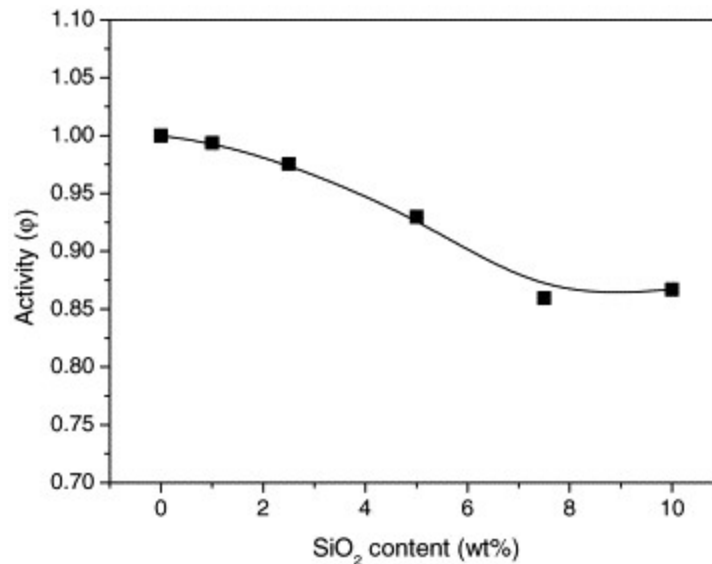


Figure 17. Variation of nucleation activity (ϕ) with silica content, for PP/SiO₂ nanocomposites

In polyamide 6, unmodified silica nanoparticles increase the crystallization rate of the matrix while modified ones decrease it [53]. In contrast, it was reported that pretreated SiO₂ nanoparticles slightly increased the non-isothermal crystallization rates of nylon 6 [54]. On the other hand, Ke et al. [55] concluded that SiO₂ particles have strong nucleation effect on PET. They investigated the nucleation and crystallization behaviors under isothermal and non-isothermal conditions of core-shell SiO₂-PS particles and their nanocomposites with PET. The nucleation rate of silica particles increased as their size decreased, being the 35 nm particles the most efficient. The spherulites grew well in PET but their size was smaller in the nanocomposites due to the silica barrier on their growth. Similarly, Huang et al. [56] determined from non-isothermal crystallization studies that γ -aminopropyltriethoxysilane treated silica nanoparticles acted as nucleating agent of

poly(ethylene-co-glycidyl methacrylate) (PEGMA). Modified Avrami model, Ozawa model, and Liu model predicted that the crystallization rate follows the order: PEGMA/Silica > PEGMA/modified-Silica > PEGMA. Calculated activation energies from Augis–Bennett model, Kissinger model and Takhor model showed that the addition of silica accelerated the crystallization process of PEGMA, whereas the silica particles also retarded the crystallization process if well dispersed.

1.3. Nanocellulose-based nanoparticles as reinforcement in polymer nanocomposites.

Cellulose is a linear homopolymer of β -(1-4)-D-glucopyranose units linked by glycosidic bond. It is comprised of microfibrils having nano size diameter and surrounded by lignin and hemicellulose [57, 58]. Cellulose is the most widely extent organic renewable material with outstanding properties and a variety of useful applications. Cellulose is also relatively inexpensive and has a much lower density than most filler that are in use today. In addition, non-plant resources can also be used to produce cellulose, especially bacteria and tunicates [59].

When subjected to acid hydrolysis, cellulose microfibrils results in a rod-like material with a relatively low aspect ratio, the nanocellulose. Due to the near perfect crystalline arrangement of cellulose whiskers, this form of nanocellulose has a high modulus and therefore significant potential as a reinforcing material. Furthermore, cellulose nanofiber has more than 200 times higher surface area than isolated cellulose fiber and possesses higher water holding capacity, higher crystallinity and higher tensile strength. Nanocellulose is a high performance nanomaterial with interesting structural and physical properties to obtain nanocomposites due to their high specific surface area, non-toxicity and biocompatibility. However, the physicochemical and structural properties of nanocellulose are found to be strongly dependent on the initial biomass type or microbial source selected, cellulose polymorphs, pretreatment process of cellulose extraction and acid hydrolysis or enzymatic treatment followed for nanocellulose fabrication[57, 58].

The reinforcement of polymers using lignocellulosic materials has been studied with the goal of obtaining fully bio-based composites. Compared to inorganic fillers, the main advantages of lignocellulosics are their renewability, low cost and low density. In addition, the important industrial problem of slow crystallization of some polymers is addressed by the use of cellulose nanocrystals as bio-based nucleation reagents. Then, another problem to solve is the difficult to disperse nanocellulose particles uniformly in polymer melts [60]. The processed method, the type of matrix and several characteristic of nanocellulose (such as physico-chemical and structural properties, surface characteristics and thermal stability) determine the dispersion quality and microstructure of polymer and then the crystallization kinetic and the final crystallinity of the matrix, and consequently affect the properties and performance of the nanocomposite.

In general, the incorporation of nanoparticles produced an increase in crystallization rate of semicrystalline polymers. In the case of nanocomposites based on PLA and microfibrillated cellulose (MFC), obtained by casting, the PLA started to crystallize earlier than neat PLA, which is an indication that the presence of MFC can act as nucleating agent on the crystallization of PLA. In addition the higher crystallinity of the composite compared to neat PLA, showed that the presence of MFC accelerates the crystallization of PLA. This can be clearly seen in the cooling scan where the thermogram shows a peak of melt crystallization temperature (T_{mc}). This T_{mc} peak of composite occurs at a higher temperature and with greater area than that of neat PLA (Figure 18)[61]. As a result of the increased crystallinity when MC is added, there is an increase in storage modulus of crystallized PLA, (the addition of 20 wt% of MFC increases the storage modulus of PLA from 293 MPa to 1034 MPa. These results demonstrated that MFC could extend the application of PLA, particularly for products exposed to high temperature.

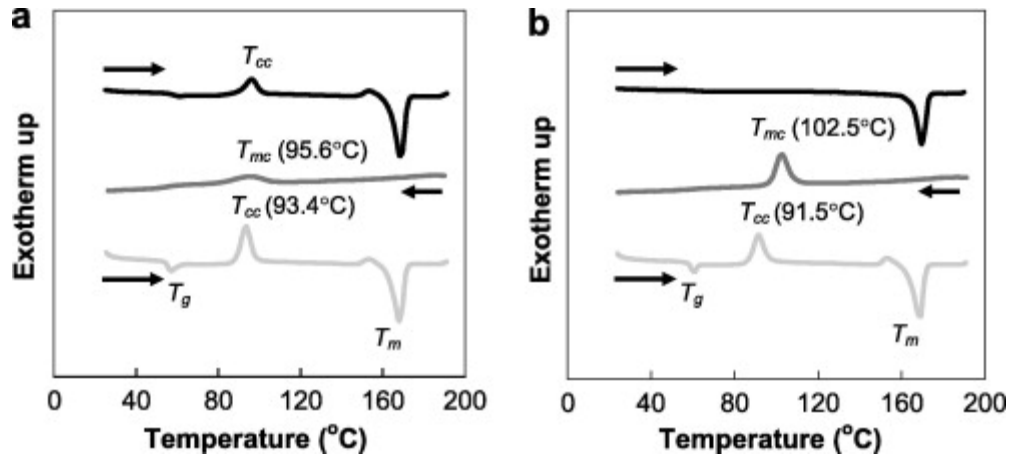


Figure 18. DSC thermogram of (a) neat PLA and (b) PLA/MFC 10 wt.% composite.

The aspect ratio of CNCs played an important role in the mechanical reinforcing efficiency and crystallization behavior of the nanocomposites. In order to analyze these effects, Dhar et al. [62] fabricated nanocomposites with PLA and cellulose nanocrystals (CNC) by extrusion, utilizing four varieties of CNC obtained by different acid treatments, which leads to different physical, structural, thermal and surface characteristics of CNC. The CNC were fabricated using different acid systems with: sulphuric acid (CNC-SO₄), phosphoric acid (CNC-PO₄), hydrochloric acid (CNC-Cl) and nitric acid (CNC-NO₃). Interestingly, the four acid-derivatized CNCs show different morphology and dimensions which led to variable aspect ratios of ~50, ~17, ~57 and ~24 for CNC-SO₄, CNC-Cl, CNC-PO₄ and CNC-NO₃ respectively. Also, the hydroxyl groups of CNCs are substituted with anionic moieties from acid which alters its interfacial interaction with PLA matrix. Then, they study the isothermal crystallization kinetics by DSC to understand the influence of variable aspect ratio and chemical functionalities of CNCs on the crystallization behavior and mechanism of the growth of spherulites of PLA. Figure 19 shows the POM micrographs at different time intervals for the PLA and 1 wt.% CNC/PLA nanocomposites, isothermally crystallized at 120°C. The isothermal crystallization kinetics was studied using the Avrami model. In general, the introduction of CNC in PLA decreases the peak time for crystallization. CNC-PO₄ and CNC-Cl show hydrophobic surface behavior which helped in improving their dispersion in the matrix and increased the number of sites for nucleation and reduced the peak crystallization time so enhancing the rate of PLA crystallization. CNCs with lower aspect ratio, such as CNC-Cl (~17) with small rod-like morphology, are

found to enhance the nucleation phenomenon during the crystallization process and accelerated the crystallization rate. Evaluation of the Avrami parameters and the crystallization half time ($t_{0.5}$) values shows that the nucleation efficiency of the various acid-derived CNCs followed the order CNC-Cl>CNC-PO₄>CNC-SO₄ and CNC-NO₃. The acid-derived CNCs showed heterogeneous nucleation with propagation of PLA spherulites in three dimensions. Lauritzen-Hoffman nucleation phenomenon shows that incorporation of CNCs into PLA matrix hindered the growth of spherulites. Then, the calculated activation energy values for different PLA/CNC systems are found to be dependent on the aspect ratio of the CNCs as well as on their compatibility with the PLA matrix. Finally, CNCs with high aspect ratio improved the elastic modulus and elongation behavior of nanocomposites. The high aspect ratio of CNC-PO₄ compared to the other acid-derived CNCs could also have led to higher reinforcement efficiency at lower volume fractions resulting in improved stress transfer from CNCs to the PLA matrix. Further, the improved elongation behavior of PLA/CNC-PO₄ is due to improved interfacial adhesion between the CNC-PO₄ and PLA matrix, which is however absent in other acid-derived CNC nanocomposites where higher degree of agglomerations are predominant. In addition the thermal stability depended of the aspect ratio of CNCs, the nanocomposites with CNC-PO₄ and CNC-NO₃ being thermally most stable followed by CNC-Cl and CNC-SO₄ respectively.

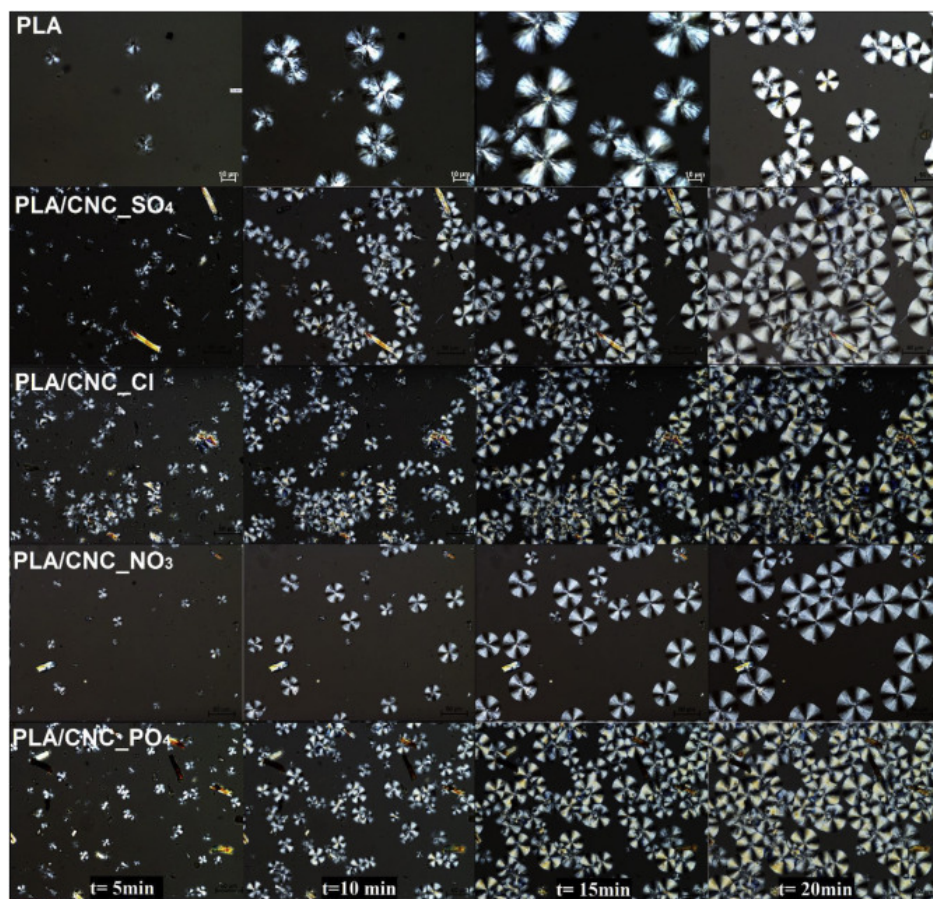


Figure 19. POM micrographs of the PLA and PLA/CNC nanocomposites fabricated with different acid hydrolyzed CNCs isothermally crystallized at TISO $\frac{1}{4}$ 120 °C taken at different time intervals (t $\frac{1}{4}$ 5, 10, 15 and 20 min).

In addition, Pei et al. [63] studied the effect of functionalized nanocellulose. For that obtained nanocomposites with poly(L-lactide) (PLLA) and two types CNC by casting, and CNC were prepared by acid hydrolysis of cotton and CNC functionalized by partial silylation (SCNC). The unmodified CNC formed aggregates in the composites, whereas the SCNC were well-dispersed and individualized in PLLA. The non-isothermal crystallization and melting behavior of the PLLA/cellulose nanocrystal composites were investigated by DSC. In the heating scans, all samples showed a distinct exothermic peak, attributing to the cold crystallization during heating process. The crystallinity of PLLA in the CNC nanocomposites was slightly increased, while the crystallinity values of PLLA in the PLLA/SCNC nanocomposites were increased considerably. In the cooling scans, the exothermic peaks with very low intensity were observed for the pure PLLA and PLLA/CNC nanocomposite samples. As for the PLLA/SCNC nanocomposite samples, the

crystallization peaks had relatively higher intensity and started from higher temperature as a result of enhanced crystallizability. The nucleation effect was remarkably enhanced when homogeneous cellulose nanocrystals dispersion in PLLA was achieved. Compared with PLLA/CNC, the PLLA/SCNC composites were nanostructured with a highly dispersed nanocrystal phase and the associated larger specific surface area for crystallite nucleation. Then, the increased degree of crystallinity and fine dispersion improved tensile modulus and strength of the nanocomposite (tensile modulus and tensile strength of the PLLA/SCNC were more than 20% higher than for pure PLLA with only 1 wt.% SCNC).

The compatibility between the hydrophobic matrix and hydrophilic CNC has been improved via surface initiated ring opening polymerization. Also, Lizundia et al.[64]obtained nanocomposites with PLLA and cellulose nanocrystals (CNC) and CNC-grafted-PLLA (CNC-g-PLLA) in order to analyze this effect. The crystallinity degree of nanocomposites remains similar to that of PLLA, but the CNC acts as nucleating agents during the crystallization process and increase the crystallization rate of PLLA. The CNC induces a greater reduction on $t_{0.5}$ than CNC-g-PLLA nanohybrid (a mean value of 4.6-fold and 2.4-fold, respectively). This matter could be associated with a surface-induced crystallization mechanism in which neat CNC are more efficient than grafted CNC. The fact that the X_c remains almost unchanged with the addition of both CNC and CNC-g-PLLA while T_m increases by 10–15⁰C suggest that the same crystalline amount is developed during crystallization, but the presence of CNC-g-PLLA and CNC (in an increasing order) result in much thicker lamella in comparison with neat polymer. In addition, T_g and T_m of nanocomposites remain ~15⁰C above from the values obtained for unreinforced polymer. Finally, results reveal a reduction on the thermal stability when in presence of CNC-g-PLLA, while raw CNC slightly increases the thermal stability of PLLA, because the presence of residual catalyst in CNC-g-PLLA plays a crucial role in the thermal degradation behavior of nanocomposites.

To study the effect of the addition of the nanocellulose on the size of the spherulite, Yu et al.[65]obtained nanocomposites of poly(3-hydroxybutyrate-co-3-hydroxyvalerate) (PHBV) with different cellulose nanocrystals (CNCs) contents, by solution casting. The crystallization behavior of PHBV and these nanocomposites was studied by DSC, wide-angle X-ray diffraction and polarized optical microscopy. They found that the CNCs act as

an effective heterogeneous nucleation agent for crystallization of PHBV, inducing an increase in the melt crystallization temperature of the nanocomposites. Then the crystallization of PHBV developed easier by incorporating well-dispersed CNCs. A study of the non-isothermal crystallization kinetics showed that overall crystallization rate of PHBV with CNC was faster than that of neat PHBV, producing a decrease in the crystallinity and the spherulite diameter of PHBV, as shown in Figure 20. However, the crystallinity decreased from 50.9% for PHBV to 44.26% for PHBV/CNC10, because the regularity of PHBV chains was disturbed by the interactions between the CNCs and PHBV matrix. Furthermore, the contact angle decreased from 60.1° for neat PHBV to 32.5° for the nanocomposites with 10% CNCs. Also, the improved hydrophilicity and the lowered crystallinity in the nanocomposites, was beneficial to the penetration of water molecule into amorphous regions, which would induce a distinct acceleration of the cleavage of PHBV side-chains and control the biodegradation rate of PHBV by adjusting the CNC contents.

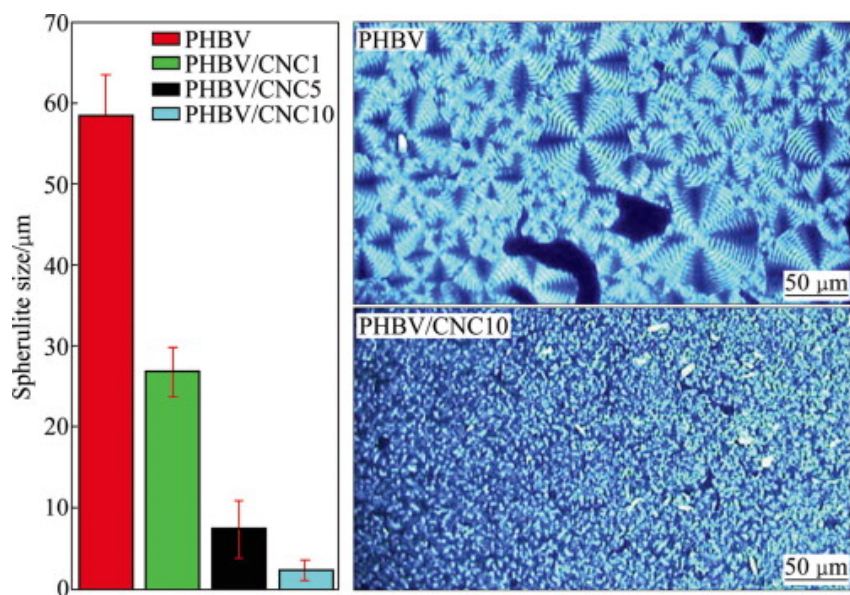


Figure 20. Spherulite size and spherulite morphologies for neat PHBV and nanocomposites with various CNC contents.

Similar results were obtained by Khoshkava et al. [66] in nanocomposites prepared via melt compounding with cellulose nanocrystal (CNC) and polypropylene (PP). It was observed by DSC that the crystallization rate of nanocomposites with 1 wt.% CNC was

faster than that of neat PP. As illustrated in Figure 21, the observation using POM confirmed the DSC results. While PP crystals are in the process of growing (Figure 21, left, top, at 48s), the formation of small crystals in PP/CNC (Figure 21, right, middle, at 50s) is almost finished. Additionally, the crystallite size and morphology are significantly different. So, PP/CNC nanocomposites could offer useful advantages in processing such as shorter cooling times in injection and blow injection molding applications. Three crystallization kinetics models: Avrami, Tobin and Malkin were employed to the DSC results. These models indicated a faster crystallization rate for PP/CNC. But, the Avrami model prediction is very close to the experimental data. In addition, the differences between experimental data and model predictions were smaller for nanocomposites than for PP. In addition, the estimated initial lamellae thickness during isothermal crystallization of PP in nanocomposites was higher than that of neat PP. This could be due to steric hurdles introduced by CNC nanoparticles, leading to a reduction in the transport of the PP chains into crystal units. As a result it is expected that crystals formed in the PP/CNC system were less perfect than those obtained with neat PP

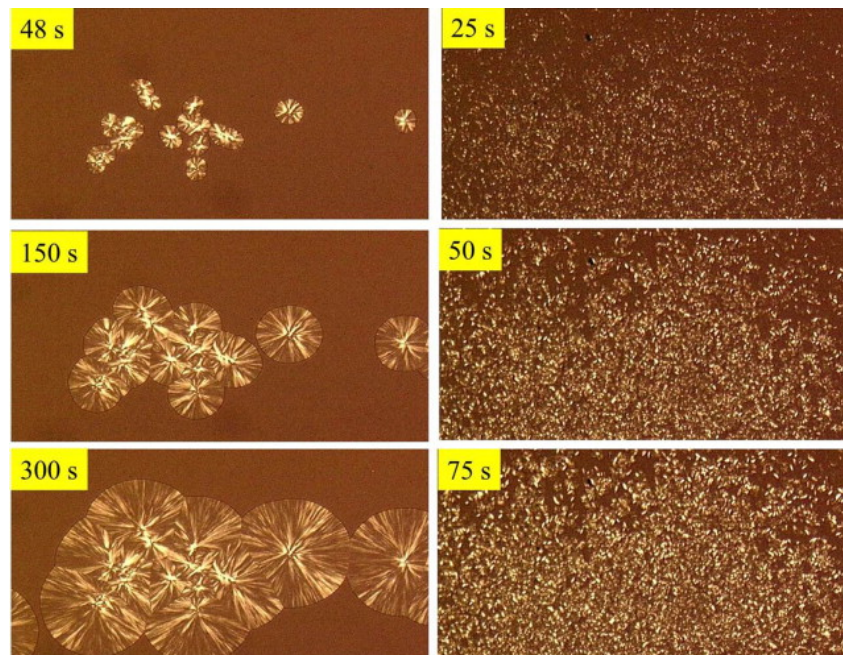


Figure 21. POM micrographs for isothermal crystallization at 126 °C for (left) PP and (right) PP/CNC.

Further, Gray et al. [67] confirmed the nucleating effect of nanocellulose on PP with the development of a transcrystalline layer, as seen by polarized optical microscopy. The image in Figure 22 shows that while the film edge enhances nucleation, the growth rate of the transcrystalline layer is about the same as that of the bulk spherulites, with the width of the layer roughly equal to the radii of the bulk spherulites. Han et al. [68], studied the morphology and crystallization properties of polyurethane/cellulose whisker nanocomposites, and determined the nucleating effect of cellulose whiskers in isothermal crystallization kinetic. In this work based on Avrami model, the cellulose whiskers leded higher crystallization rate and promoted heterogeneous crystallization and crystal growth in two dimensions. The faster crystallization of the neat polyurethane in presence of cellulose fillers correlated with the lower activation of energy as assessed from Avrami model.

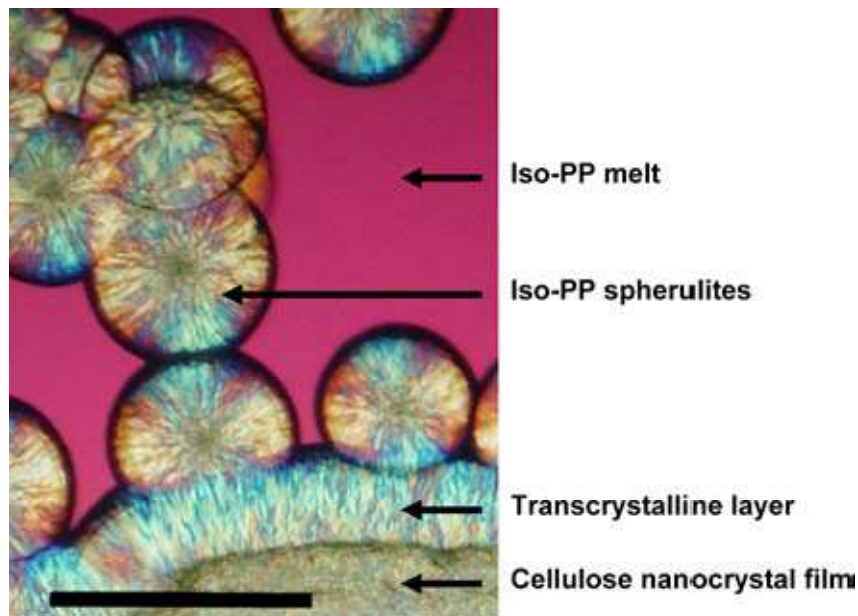


Figure 22. Edge of cellulose nanocrystal film in contact with isotactic polypropylene melt at higher magnification. Crossed polars, first-order red plate. Scale bar, 200 μm

In addition, Ten et al. [69] prepared PHBV films with different amounts of cellulose nanowhiskers (CNWs) by solution casting. Crystallization behaviors were studied under isothermal conditions using DSC and POM. The crystallization kinetics combining nucleation and growth effect was analyzed using the Avrami equation, in order to study the effects of CNW concentration and temperature on the crystallization rate and crystallinity

of PHBV. The nanowhiskers did not cause new crystalline symmetries of PHBV. But the results showed that the apparent crystal size D_{hkl} , determined using Scherer's equation, was smaller in the composites than in the pure PHBV, implying that CNWs hindered the diffusion and folding of PHBV chains due to the confinement effects of the nanowhiskers. Additionally, the nanocomposites with low concentrations of CNWs presented the smallest D_{hkl} , because CNWs were homogeneously dispersed in PHBV. Moreover, the refined crystal structures could contribute to improved mechanical properties of the composites. The results showed the dual effects: nucleation and confinement of CNWs. Depending on the concentration of CNWs, the crystallization rate of PHBV could be either increased or decreased due to the combined effects. In addition, high crystallization temperatures increased the diffusion rate of PHBV chains and the growth rate of PHBV spherulites. However, the nucleation effect of CNWs decreased at high crystallization temperatures. The resulting effect is reflected in the overall crystallization rate shown in the Figure 23. These results were confirmed by the spherulite growth rate and nucleation density estimated from POM studies.

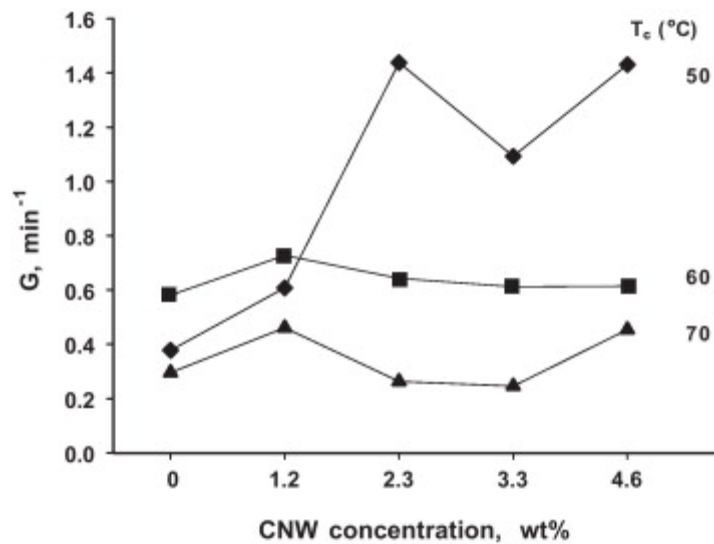


Figure 23. Overall crystallization rate G of PHBV and PHBV/CNW composites at different crystallization temperatures.

A comparative performance study of cellulose whiskers (CW) and starch nanoparticles (SN) on plasticized starch (PS) has been done. The nanocomposites were

prepared by casting in water, with glycerol as plasticizer. PS present more affinity to the CW than SN. Additionally, near-perfect crystalline structure of CWs provided an efficient nucleating agent for transcrystallization, which was corroborated by X-ray diffraction. Nanocomposites SNs showed higher reinforcement in dynamic mechanical tests compared to the nanocomposites containing CWs, which were attributed to more efficient filler/filler and filler/matrix interactions originated from hydrogen bonding in SN-filled nanocomposites[70].

In order to improve the final properties of poly(hydroxybutyrate) (PHB) and poly(lactic acid) (PLA), Arrieta et al.[71] obtained nanocomposites with PLA and PHB blends with cellulose nanocrystals (CNC). Cellulose nanocrystals and surfactant modified cellulose nanocrystals (CNCs) were synthesized from microcrystalline cellulose by acid hydrolysis. PHB increased the crystallinity of PLA due to its nucleation effect. Then, the overall crystallinity was increased in the PLA–PHB blend by the addition of CNC and more with the addition of modified CNCs. The incorporation of surfactant modified cellulose nanocrystals into PLA–PHB blends was effective to improve the compatibility between both polymers processed by means of a simple melt-blending process.

Mathew et al. [72] prepared nanocomposites from waxy maize starch plasticized with sorbitol as the matrix and tunicin whiskers. The system exhibited a single glass rubber transition, and was no evidence of transcrystallization of amylopectin on cellulose whisker surfaces. When whiskers were added to the plasticized starch matrix, they get homogeneously dispersed in the system. A significant increase in crystallinity was observed in the composites by increasing either moisture or whiskers content. This phenomenon resulted most probably from a nucleating effect of the filler. The Tg of the plasticized starch matrix increased slightly. This was ascribed to the presence of stiff crystalline whiskers and to the increase of crystallinity upon whisker addition, both resulting in a restriction of the mobility of amorphous amylopectin chains.

Additionally, Masa et al. [73] studied nanocomposites of poly(oxyethylene) (PEO) reinforced with cellulose nanocrystals. It was found that the degree of crystallinity of the nanocomposite films is constant up to 10 wt.% whiskers, but decreases at higher whisker contents. Figure 24 shows DSC thermograms of the dynamic cooling crystallization of the PEO matrix and 10 and 30 wt% tunicin whiskers based composites. Crystallization

temperature and the temperature associated with the beginning of the crystallization process decrease as the cellulose whiskers content increases. It could be ascribed to an anti-nucleation effect of the filler, due to favorable interactions between cellulose and PEO, resulting in a restricted molecular mobility of PEO chains in contact with the whiskers and then an increase of the viscosity of the polymer melt that induce an increase of the activation energy of diffusion of the chains. And finally a decrease of the crystallinity of PEO was observed. The chief effect of the filler was a thermal stabilization of the storage modulus for the composites above the melting temperature of the matrix. This phenomenon was well predicted from a model based on the percolation concept. It was also suggested that the cellulose nanocrystals exhibited a nucleating effect.

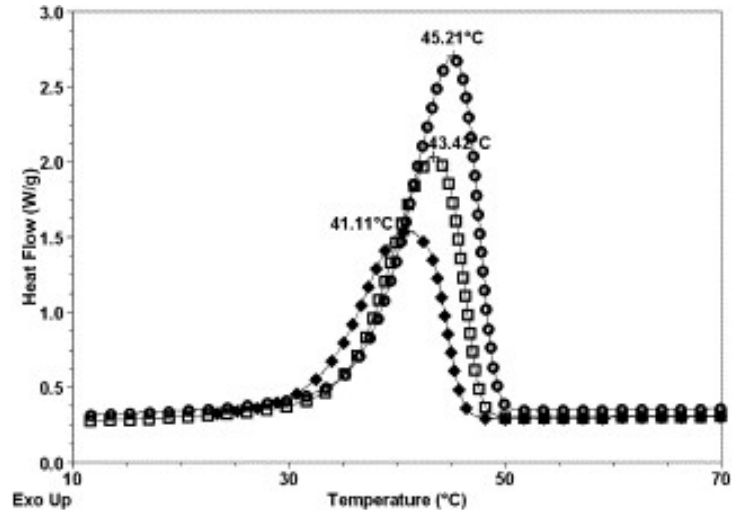


Figure. 24. DSC thermograms showing the non-isothermal crystallization at 10 °C/min for PEO based composites filled with 0 (○), 10 (□) and 30 wt% (◇) of tunicin whiskers.

Rahimi et al. [74] studied the effect of CNC and aminopropyltriethoxysilane (APS) - modified CNC nanocomposites on non-isothermal crystallization behavior of PA6. Their results showed that the CNC developed a network-like fibrillar structure while the APS was finely dispersed. The addition of CNCs resulted in longer crystallization half-times and reduction in Avrami rate constant, indicating a hindrance effect of the cellulose nanocrystals on the crystallization process, in accordance with corresponding fibrillar microstructure. On other hand, the APS particles improved the nucleation activity and

increased the Avrami (K) constant, as can be seen in the isothermal thermograms at 194⁰C, Figure 25. The effect of nucleation activity of the surface modified CNCs was confirmed by the Hoffman theory and polarized optical micrographs. From the non-isothermal crystallization analysis, it was observed that the APS-modified CNCs shifted the crystallization peak and its onset temperature towards higher temperatures while an opposite effect was observed for the non-modified CNCs. By contrast, a study by Kiziltas et al. [75] showed that incorporation of microcrystalline cellulose (MCC) into polyamide 6 reduced the overall crystallinity of the matrix. The onset and peak crystallization temperature of the PA6 was shifted towards relatively larger values. But, the analysis of the non-isothermal crystallization of these systems via Avrami and Tobin models, showed no significant changes.

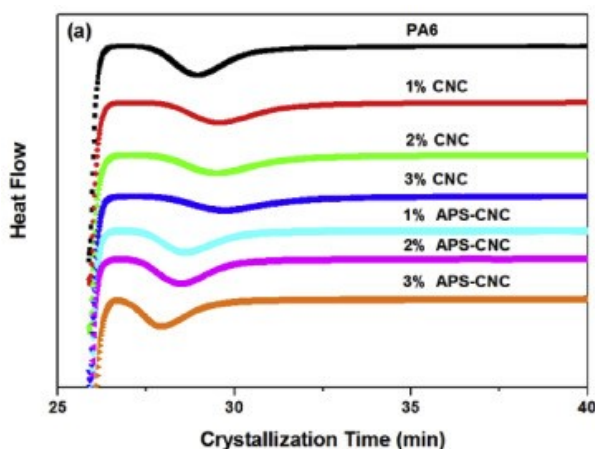


Figure 25. Isothermal crystallization exotherms at 194⁰C.

The effect of cellulose particles on the crystallization/melting behavior of polycaprolactone (PCL) was studied by Siqueira et al.[76]. The nanocomposites were prepared by mixing PCL with surface modified sisal nanowhiskers (CNW) and microfibrillated cellulose (MFC) extracted from sisal fibers. Finally, the isothermal crystallization data were modeled with Avrami's kinetics, Lauritzen–Hoffman secondary nucleation theory and equilibrium melting points were determined with the Hoffman–Weeks method. The modified MFC was more hydrophobic than the modified CNWs. It results that MFC should be better dispersed in PCL matrix. However, the presence of those two cellulosic nanoparticles increases the degree of crystallinity of PCL matrix. Then, the

cellulose nanoparticles, acting as nucleating agents, accelerate the crystallization of PCL while depressing its equilibrium melting, as can be clearly seen in Figure 26. In addition, the crystallization of MFC-nanocomposites was slightly faster than that of CNW-nanocomposites, in agreement with the slightly lower bulk activation energy for crystallization and nucleation parameter in the first. The increase in crystallinity which was more pronounced with CNWs is consistent with the cellulose nucleating effect and the greater surface area available with CNWs for heterogeneous nucleation.

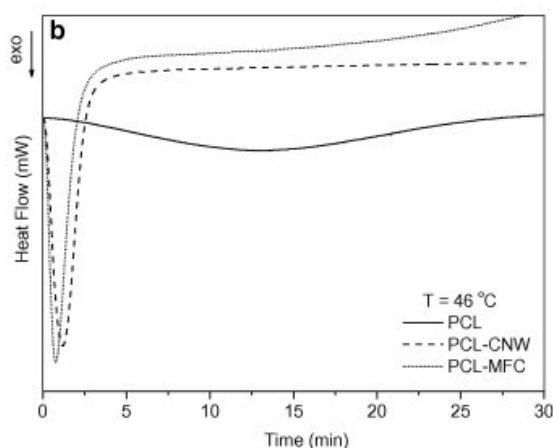


Figure 26. Crystallization exotherms for pure PCL and PCL–nanocomposites reinforced with 12 wt% of modified sisal CNW or modified sisal MFC crystallized at $T_c = 46^{\circ}\text{C}$.

Ghadikolaei et al.[77] studied the non-isothermal crystallization kinetics and morphology of the ethylene–vinyl acetate copolymer/bacterial cellulose nanofiber (EVA/BCN) nanocomposites, fabricated via solution casting method. The neat EVA and EVA/BCN nanocomposites presented the same crystal structure via X-ray diffraction and the BC fibers dispersed well in the EVA matrix, according to TEM investigation. The kinetic of crystallization was studied by DSC, and various kinetic methods were used to determine the kinetic parameters of crystallization under non-isothermal condition, such as Jeziorny, Ozawa, Mo and Flynn–Wall–Ozawa (FWO) theories. The EVA/BCN 3 wt.% had the highest relative crystallinity at the same crystallization time, and the relative crystallinity of the EVA/BCN (1 and 5 wt.%) was lower than that of the neat EVA (Figure 27). The results of kinetic parameters, such as half crystallization time ($t_{0.5}$), crystallization rate constant (Z_c), and activation energy (E_a) revealed that the crystallization process was slightly enhanced by the presence of only 3 wt.% BCNs. The Jeziorny, Mo and FWO

models could successfully describe the crystallization kinetics of EVA/BCN nanocomposites. But the Ozawa model described the non-isothermal process only at relatively low cooling rates.

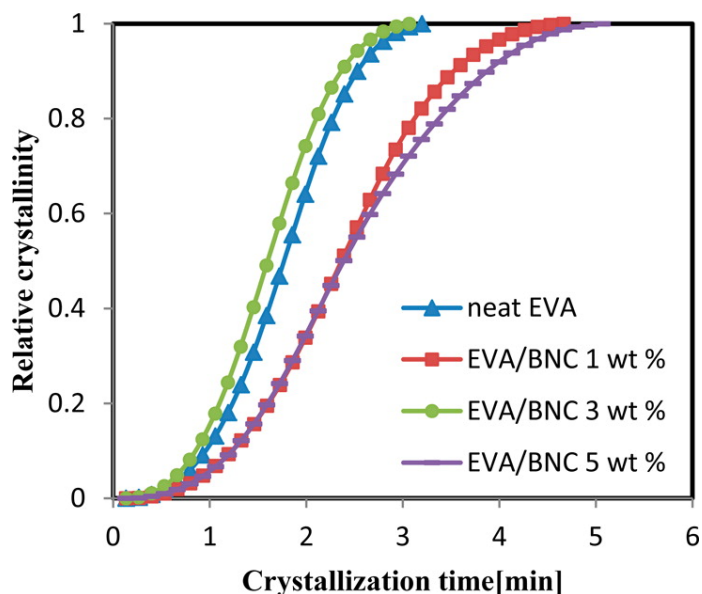


Figure 27. Plots of relative crystallinity versus time for the pure EVA and EVA/BCN (1, 3, and 5 wt.%) nanocomposites at 2.5 °C/min.

2. Concluding remarks

Thermal, physical and mechanical properties of a semicrystalline polymer are significantly influenced by crystallinity and crystalline morphology. Nanoparticles can influence their crystallization behaviour. Moreover, polymer nanocomposites have been extensively studied in the literature as an effective approach towards modulating the physical and structural properties of the neat polymers. So, the knowledge of the parameters affecting crystallization is crucial for the optimization of the processing conditions and the final properties of the materials. Usually, studies on crystallization behavior of polymers include crystallization temperature, crystal shapes, isothermal and non-isothermal crystallization kinetics. Particularly, it is important to study crystallization

kinetics for understanding the details on crystallization behavior of polymeric nanocomposites and then, predict the material behavior.

Mostly, it was reported that the nanoparticles can serve as heterogeneous nucleation sites for crystallization and act as effective nucleating agents. However, their effect on the crystallization rate is still controversial since it was found that some fillers decreased the nucleation activity when a good dispersion and miscibility with the polymer matrix were achieved. In general, the overall crystallization process is expected to be accelerated due to the heterogeneous nucleation process. However, nanoparticles can also hinder the molecular chain mobility and consequently delay crystallization rate. Then, the competition between the nucleation effect and polymer chain retardation determines the whole crystallization process.

Depending on the shape, specific surface area and functionalization of nanoparticles as well as their dispersion in the matrix both nucleation and crystallization rate, can be affected.

Well known crystallization kinetics models were used in several works to analyze the effect of nanoparticle addition on the polymer crystallization. These theories were also widely used to predict crystallization during processing, because the resulting physical properties of the polymer are strongly related to the morphology and the extent of crystallization. It would be possible to reduce the processing time if the addition of nanoparticles provides more nucleation sites, thus resulting in an increase in the overall crystallization rate.

3. Acknowledgement

The authors gratefully acknowledge the support from the Consejo Nacional de Investigaciones Científicas y Técnicas, CONICET (PIP 0527) and ANCyPT (PICT12-1983) and the Universidad Nacional de Mar del Plata.

4. References

- [1] Deshmukh, G.S., Peshwe, D.R., Pathak, S.U., Ekhe, J.D. 2015. Nonisothermal crystallization kinetics and melting behavior of poly(butylene terephthalate) and calcium carbonate nanocomposites. *Thermochim Acta*. 606, 66–76.
- [2] Olmos, D., Domínguez, C., Castrillo, P.D., Gonzalez-Benito, J. 2009. Crystallization and final morphology of HDPE: Effect of the high energy ball milling and the presence of TiO₂ nanoparticles. *Polymer*. 50, 1732–1742.
- [3] Ma, D., Akpalu, Y. A., Li, Y., Siegel, R.W., Schadler, L.S. 2005. Effect of Titania Nanoparticles on the Morphology of Low Density Polyethylene. *J PolymSci Pol Phys*. 43, 488–497.
- [4] Mandalia, T., Bergaya, F. 2006. Organo clay mineral–melted polyolefin nanocomposites Effect of surfactant/CEC ratio. *J PhyChem Solids*. 67, 836-845.
- [5] Drown, E.K., Mohanty, A.K., Parulekar, Y., Hasija, D., Harte, B.R., Misra, M., Kurian, J.V. 2007. The surface characteristics of organoclays and their effect on the properties of poly(trimethylene terephthalate) nanocomposites. *Composites Sci Technol*. 67, 3168-3175.
- [6] Hedley, C.B., Yuan, G., Theng, B.K.G. 2007. Thermal analysis of montmorillonites modified with quaternary phosphonium and ammonium surfactants. *Appl Clay Sci*. 35, 180-188.
- [7] Fornes, T.D., Yoon, P.J., Keskkula, H., Paul, D.R. 2001. Nylon 6 nanocomposites: the effect of matrix molecular weight. *Polymer*. 42, 9929-9940.
- [8] Murray, H.H., 1991. Overview–clay mineral applications. *Appl Clay Sci* 5, 379–95.
- [9] Roelofs, J.C.A.A., Berben, P.H. 2006. Preparation and performance of synthetic organoclays. *Appl Clay Sci*. 33, 13-20.

- [10] Capková, P., Pospíši, M., Valášková, M., Merínská, D., Trchová, M., Sedláková, Z., Weiss, Z., Šimoník, J. 2006. Structure of montmorillonite intercalated with stearic acid and octadecylamine: Modeling, diffraction, IR spectroscopy. *J Colloid Interf Sci.* 300, 264–269.
- [11] D’Amico, D.A., Cyras, V.P., Manfredi, L.B. 2014. Non-isothermal crystallization kinetics from the melt of nanocomposites based on poly(3-hydroxybutyrate) and modified clays. *ThermochimActa.* 594, 80–88,
- [12] D’Amico, D.A., Manfredi, L.B., Cyras, V.P. 2012. Crystallization behavior of poly(3-hydroxybutyrate) nanocomposites based on modified clays: Effect of organic modifiers. *Thermochim Acta.* 544, 47– 53
- [13] Daitx T.S., Carli L. N., Crespo J. S., Mauler R.S. 2015. Effects of the organic modification of different clay minerals and their application in biodegradable polymer nanocomposites of PHBV. *Appl Clay Sci.* 115, 157–164.
- [14] Lai S-M., Wu Sh-H., Lin G-G., Don T-M. 2014. Unusual mechanical properties of melt-blended poly(lactic acid) (PLA)/clay nanocomposites. *EurPolym J.* 52, 193–206.
- [15] Picard, E., Espuche, E., Fulchiron, R. 2011. Effect of an organo-modified montmorillonite on PLA crystallization and gas barrier properties. *Appl Clay Sci.* 53, 58–65.
- [16] Krikorian V., Pochan D. 2004. Unusual Crystallization Behavior of Organoclay Reinforced Poly(L-lactic acid) Nanocomposites, *Macromolecules.* 37, 6480-6491.
- [17] Krikorian V., Pochan, D.J. 2005. Crystallization Behavior of Poly(L-lactic acid) Nanocomposites: Nucleation and Growth Probed by Infrared Spectroscopy. *Macromolecules.* 38, 6520-6527.

- [18] Smith, L., Vasanthan, N. 2015. Effect of clay on melt crystallization, crystallization kinetics and spherulitic morphology of poly(trimethyleneterephthalate) nanocomposites. *ThermochimActa*. 617, 152–162.
- [19] Papageorgiou, G.Z., Karandrea, E., Giliopoulos, D., Papageorgiou, D.G., Ladavos, A., Katerinopoulou, A., Achilias, D. S., Triantafyllidis, K. S., Bikiaris, D. N. 2014. Effect of clay structure and type of organomodifier on the thermal properties of poly(ethylene terephthalate) based nanocomposites. *ThermochimActa*. 576, 84– 96.
- [20] Cao, T., Feng, Y., Chen, G., Guo, C-Y. 2014. Effect of photofunctionalorgano anion-intercalated layered double hydroxide nanoparticles on poly(ethylene terephthalate) nonisothermal crystallization kinetics. *ReactFunctPolym*. 83, 1–6.
- [21] Perez, C.J., Alvarez, V.A. 2009. Overall Crystallization Behavior of Polypropylene–Clay Nanocomposites; Effect of Clay Content and Polymer/Clay Compatibility on the Bulk Crystallization and Spherulitic Growth. *J ApplPolym Sci*. 114, 3248–3260.
- [22] Hu, D., Chen, J., Zhao, L., Liu, T. 2015. Melting and non-isothermal crystallization behaviors of polypropylene and polypropylene/montmorillonitenanocomposites under pressurized carbon dioxide. *ThermochimActa*. 617, 65–75.
- [23] Yuan, Q., Awate, S., Misra, R. D. K. 2006. Nonisothermal Crystallization Behavior of Melt-Intercalated Polyethylene-Clay Nanocomposites. *J ApplPolym Sci*. 102, 3809–3818.
- [24] Tjong, S.C., Bao, S.P. 2005. Crystallization Regime Characteristics of Exfoliated Polyethylene/Vermiculite Nanocomposites. *J PolymSci Pol Phys*. 43, 253–263.
- [25] Panupakorn, P., Chaichana, E., Prasertthdam, P., Jongsomjit, J. 2013. Polyethylene/Clay Nanocomposites Produced by In Situ Polymerization with Zirconocene/MAO Catalyst” *Journal of Nanomaterials*. Article ID 154874, 9 pages.

- [26] Maiti, P., Okamoto, M. 2003. Crystallization Controlled by Silicate Surfaces in Nylon 6-Clay Nanocomposites. *Macromol. Mater Eng.* 288, 440–445.
- [27] Katoh, Y., Okamoto, M. 2009. Crystallization controlled by layered silicates in nylon 6–clay nano-composite. *Polymer.* 50, 4718–4726.
- [28] Dobreva, A., Gutzow, I. 1993. Activity of substrates in the catalyzed nucleation of glass-forming melts. I. Theory. *J. Non-Cryst.Solids.* 62, 1-12.
- [29] Xia, X., Cai, S., Xie, Ch. (2006) Preparation, structure and thermal stability of Cu/LDPE nanocomposites. *Mater Chem Phys.* 95, 122–129.
- [30] Huang, Z., Wang, S., Kota, S., Pan, Q., Barsoum, M.W., Li, Ch.Y. 2016. Structure and crystallization behavior of poly(ethylene oxide)/Ti₃C₂T_x MXene nanocomposites. *Polymer.* 102, 119-126.
- [31] Chen, E-CH., Wu, T-M. 2008. Isothermal and Nonisothermal Crystallization Kinetics of Nylon 6/Functionalized Multi-Walled Carbon Nanotube Composites. *J PolymSci Pol Phys.* 46, 158–169.
- [32] Zeng, R-T., Hu, W., Wang, M., Zhang, S.-D., Zeng, J.-B. 2016. Morphology, rheological and crystallization behavior in noncovalently functionalized carbon nanotube reinforced poly(butylsuccinate) nanocomposites with low percolation threshold. *Polym Test.* 50, 182-190.
- [33] Li, J., Fang, Z., Tong, L., Gu, A., Liu, F. 2006. Effect of multi-walled carbon nanotubes on non-isothermal crystallization kinetics of polyamide 6. *EurPolym J.* 42, 3230–3235.
- [34] Lin, S-Y., Chen, E-Ch., Liu, K-Y., Wu, T-M. 2009. Isothermal Crystallization Behavior of Polyamide 6,6/Multiwalled Carbon Nanotube Nanocomposites. *PolymEng Sci.* 49(12), 2447–2453.

- [35] Haggenueller, R., Fischer, J.E., Wine, K.I. 2006. Single Wall Carbon Nanotube/Polyethylene Nanocomposites: Nucleating and Templating Polyethylene Crystallites. *Macromolecules*. 39, 2964-2971.
- [36] Kim, J.Y., Han, S.I., Kim, D.K., Kim, S.H. 2009. Mechanical reinforcement and crystallization behavior of poly(ethylene 2,6-naphthalate) nanocomposites induced by modified carbon nanotube. *Composites: Part A*. 40, 45–53.
- [37] Chatterjee, T., Lorenzo, A. T., Krishnamoorti, R. 2011. Poly(ethylene oxide) crystallization in single walled carbon nanotube based nanocomposites: Kinetics and structural consequences. *Polymer*. 52, 4938-4946.
- [38] Lim, J. Y., Kim, J., Kim, S., Kwak, S., Lee, Y., Seo, Y. 2015. Nonisothermal crystallization behaviors of nanocomposites of poly(vinylidene fluoride) and multiwalled carbon nanotubes. *Polymer*. 62, 11-18.
- [39] Wu, T-M., Chen, E.-Ch. 2006. Crystallization Behavior of Poly(ϵ -caprolactone)/Multiwalled Carbon Nanotube Composites. *J PolymSci Pol Phys*. 44, 598–606.
- [40] Jana, R.N., Cho, J. W. 2010. Non-isothermal crystallization of poly(ϵ -caprolactone)-grafted multi-walled carbon nanotubes. *Composites: Part A*. 41, 1524–1530.
- [41] Tan, L., Chen, Y., Zhou, W., Ye, S., Wei, J. 2011. Novel approach toward poly(butylene succinate)/single-walled carbon nanotubes nanocomposites with interfacial-induced crystallization behaviors and mechanical strength. *Polymer*. 52, 3587-3596.
- [42] Papageorgiou, D.G., Zhuravlev, E., Papageorgiou, G.Z., Bikiaris, D., Chrissafis, K., Schick, Ch. 2014. Kinetics of nucleation and crystallization in poly(butylene succinate) nanocomposites. *Polymer*. 55, 6725-6734.

- [43] Xu, C., Qui, Z. 2009. Isothermal Melt Crystallization Kinetics Study of Biodegradable Poly(3-hydroxybutyrate)/Multiwalled Carbon Nanotubes Nanocomposites. *Polym J.* 41, 888–892.
- [44] Avella, M., Cosco, S., Di Lorenzo, M.L., Di Pace, E., Errico, M.E. 2005. Influence of CaCO₃ nanoparticles shape on thermal and crystallization behavior of isotactic polypropylene based nanocomposites. *J Therm Anal Calorim.* 80, 131–136.
- [45] Supaphol, P., Harnsiri, W., Junkasem, J. 2004. Effects of calcium carbonate and its purity on crystallization and melting behavior, mechanical properties, and processability of syndiotactic polypropylene, *J Appl Polym Sci.* 92, 201–212.
- [46] Avella, M., Cosco, S., Di Lorenzo, M.L., Di Pace, E., Errico, M.E., Gentile, G. 2006. Nucleation activity of nanosized CaCO₃ on crystallization of isotactic polypropylene, in dependence on crystal modification, particle shape, and coating, *Eur Polym J.* 42, 1548–1557.
- [47] Wan, W., Yu, D., Guo, X., Xie, Y. 2008. Effect of nanoparticle surface treatment on nonisothermal crystallization behavior of polypropylene/calcium carbonate nanocomposites, *Polym Plast Technol Eng.* 47, 433–442.
- [48] Huang, J.W., Wen, Y.L., Kang, C.C., Tseng, W.J., Yeh, M.Y. 2008. Nonisothermal crystallization of high density polyethylene and nanoscale calcium carbonate composites, *Polym Eng Sci.* 48, 1268–1278.
- [49] Run, M., Yao, C., Wang, Y., Song, H. 2008. Nonisothermal crystallization behavior and crystals morphology of poly(trimethylene terephthalate)/nano-calcium carbonate composites, *Polym Compos.* 29, 1235–1243.

- [50] Di Lorenzo, M.L., Errico, M.E., Avella, M. 2002. Thermal and morphological characterization of poly(ethylene terephthalate)/calcium carbonate nanocomposites, *J Mater Sci.* 37, 2351–2358.
- [51] Rong, M.Z., Zhang, M.Q., Zheng, Y.X., Zeng, H.M., Walter, R., Friedrich, K. 2001. Structure–property relationships of irradiation grafted nano-inorganic particle filled polypropylene composites. *Polymer.* 42, 167-183.
- [52] Papageorgiou, G.Z., Achilias, D.S., Bikiaris, D.N., Karayannidis, G.P. 2005. Crystallization kinetics and nucleation activity of filler in polypropylene/surface-treated SiO₂ nanocomposites. *ThermochimActa.* 427, 117–128.
- [53] Yang, F., Ou, Y., Yu, Z. 1998. Polyamide 6/silica nanocomposites prepared by in situ polymerization, *J ApplPolym Sci.* 69, 355-361.
- [54] Li, Y., Yu, J., Guo, Z.X., 2003. The influence of interphase on nylon-6/nano-SiO₂ composite materials obtained from in situ polymerization. *Polym. Int.* 52 (6) 981-986.
- [55] Ke, Y.-Ch., Wu, T.-B., Xia, Y.-F. 2007. The nucleation, crystallization and dispersion behavior of PET-monodisperse SiO₂ composites. *Polymer.* 48, 3324-3336.
- [56] Huang, J.-W., Kang, Ch.-Ch., Li, Ch.-J., Lee, Ch.-T. 2005. Non-isothermal Crystallization of Poly(ethylene-co-glycidyl methacrylate)/ Silica Nanocomposites. *Polym J.* 37 (6), 418–428.
- [57] Habibi, Y., Lucia, L.A., Rojas, O.J. 2010. Cellulose nanocrystals: chemistry, self-assembly, and applications. *Chemical Reviews*, 110, 3479–3500.
- [58] Moran, J.I., Alvarez, V.A., Cyras, V.P., Vázquez, A., 2008. Extraction of cellulose and preparation of nanocellulose from sisal fibers. *Cellulose* 15, 149–159.

- [59] Masa, S., Alloin, F., Dufresne, A. 2005. Review of recent research into cellulosic whiskers, their properties and their application in nanocomposite field. *Biomacromolecules*.6, 612–26.
- [60] Mohanty, A.K., Misra, M., Drzal, L.T., 2002. Sustainable bio-composites from renewable resources: opportunities and challenges in the green materials world. *J Polym Environ*. 9(2), 19–26.
- [61] Suryanegara, L., Nakagaito, A. N., Yan, H. 2009. The effect of crystallization of PLA on the thermal and mechanical properties of microfibrillated cellulose-reinforced PLA composites. *Compos Sci Technol*. 69, 1187–1192.
- [62] Dhar, P., Mohan Bhasney, S., Kumar, A., Katiyar, V. 2016. Acid Functionalized Cellulose Nanocrystals I and its Effect on Mechanical, Thermal, Crystallization and Surfaces Properties of Poly (lactic acid) Bionanocomposites Films: A Comprehensive Study. *Polymer*. 101, 75-92.
- [63] Pei, A., Zhou, Q., Berglund, L.A. 2010. Functionalized cellulose nanocrystals as biobased nucleation agents in poly(L-lactide) (PLLA) – Crystallization and mechanical property effects. *Compos Sci Technol*. 70, 815–821.
- [64] Lizundia, J.L. Vilas, L.M. León. 2015. Crystallization, structural relaxation and thermal degradation in Poly(l-lactide)/cellulose nanocrystal renewable nanocomposites. *Carbohydr Polym*. 123, 256–265.
- [65] Yu, H.-Y., Qin, Z.-Y., Zhou, Z. 2011. Cellulose nanocrystals as green fillers to improve crystallization and hydrophilic property of poly(3-hydroxybutyrate-co-3-hydroxyvalerate). *Prog Nat Sci*. 21, 478-484.

- [66] Khoshkava, V., Ghasemi, H., Kamal, M.R. 2015. Effect of cellulose nanocrystals (CNC) on isothermal crystallization kinetics of polypropylene. *ThermochimActa*. 608, 30–39.
- [67] Gray, D.G. 2008. Transcrystallization of polypropylene at cellulose nanocrystal surfaces. *Cellulose*. 15, 297–301.
- [68] Han J., Zhu Y., Hu J., Luo H., Yeung L-Y., Li W. 2012. Morphology, reversible phase crystallization, and thermal sensitive shape memory effect of cellulose whiskers/SMPU nano-composites. *J ApplPolym Sci*. 123 (2), 749–762.
- [69] Ten, E., Jiang, L., Wolcott, M.P. 2012. Crystallization kinetics of poly(3-hydroxybutyrate-co-3-hydroxyvalerate)/cellulose nanowhiskers composites. *CarbohydPolym*. 90, 541–550.
- [70] Nasser, R., Mohammadi, N. 2014. Starch-based nanocomposites: A comparative performance study of cellulose whiskers and starch nanoparticles. *CarbohydPolym*. 106, 432–439.
- [71] Arrieta, M.P., Fortunati, E., Dominici, F., Rayón, E., López, J., Kenny, J.M. 2014. Multifunctional PLA–PHB/cellulose nanocrystal films: Processing, structural and thermal properties. *CarbohydPolym*. 107, 16–24.
- [72] Mathew, A.P., Dufresne, A., 2002. Morphological investigation of nanocomposites from sorbitol plasticized starch and tunicin whiskers. *Biomacromolecules*. 3, 609–17.
- [73] Masa, S., Alloin F., Sanchez J.Y., Dufresne A. 2004. Cellulose nanocrystals reinforced poly(oxyethylene). *Polymer*. 45, 4149–57.
- [74] Rahimi, S.K., Otaigbe, J.U. 2016. The role of particle surface functionality and microstructure development in isothermal and non-isothermal crystallization behavior of polyamide 6/cellulose nanocrystals nanocomposites. *Polymer*. 107, 316–331.

- [75] Kiziltas, A., Nazari, B., Gardner, D.J., Bousfield, D.W. 2013. Polyamide 6–cellulose composites: Effect of cellulose composition on melt rheology and crystallization behavior. *Polym Eng Sci.* 54 (4), 739-746.
- [76] Siqueira, G., Frascini, C., Bras, J., Dufresne, A., Prud'homme, R., Laborie, M.-P. 2011. Impact of the nature and shape of cellulosic nanoparticles on the isothermal crystallization kinetics of poly(ϵ -caprolactone). *EurPolym J.* 47, 2216–2227.
- [77] Ghadikolaei, S.S., Omrani, A., Ehsani, M. 2016. Impact of Bacterial Cellulose Nanofibers on the Nonisothermal Crystallization Kinetics of Ethylene–Vinyl Acetate Copolymer. *Ind. EngChem Res.* 55, 8248–8257.